Rivista Italiana di Paleontologia e Stratigrafia	volume 118	no. 3	2 pls.	pp. 439-460	November 2012

CALCAREOUS NANNOFOSSIL BIOSTRATIGRAPHY OF THE S'ADDE LIMESTONE (MT. ALBO, OROSEI GULF): INSIGHTS INTO THE MIDDLE-LATE JURASSIC EASTERN SARDINIA PASSIVE MARGIN EVOLUTION

CRISTINA EMANUELA CASELLATO [1], FLAVIO JADOUL [1] & ALESSANDRO LANFRANCHI [2]

Received: February 9, 2012; accepted: June 26, 2012

Key words: Callovian-Early Tithonian, Eastern Sardinia, S'Adde Limestone, Calcareous nannofossil, Hardground; South European passive margin.

Abstract. Calcareous nannofossil biostratigraphy has been performed on 3 sections cropping out in Eastern Sardinia (Orosei Gulf, Mt. Albo). Calcareous nannofossils are rare to few and poorly to moderately preserved. Nevertheless thirteen bioevents have been recognized (S'Adde valley section) and a Late Bathonian-Early Tithonian age is derived for the S'Adde Limestone (Lms.). The inferred age constraints, integrated with data from the literature, allow the revision of the S'Adde Lms. chronostratigraphy, and the formalization of the *S'Adde Limestone* (Dieni & Massari 1985) as a lithostratigraphic unit.

Qualitative evaluations of carbonate production/sedimentation rates for the north Mt. Albo area are proposed: the Late Bathonian-Callovian and Oxfordian were times of pronounced reduction of carbonate production/exportation, in agreement with the European passive margin evolution, also affected by starvation fenomena and condensations.

A Middle-Late Jurassic basin-and-swell setting related to regional tensional tectonic activity is reconstructed for the north Mt. Albo area. The comparison of new and literature data allows framing the local and Eastern Sardinia passive margin evolution in the broader geodynamic and paleogeographic context of the southern European margin.

Riassunto. In questo studio sono state condotte analisi biostratigrafiche a nannofossili calcarei su tre sezioni stratigrafiche affioranti nella Sardegna Orientale (Golfo di Orosei, Massiccio del M.te Albo). I nannofossili calcarei sono rari e presentano conservazione da scarsa a moderata, ma è stato comunque possibile riconoscere (sezione della Valle di S'Adde) tredici eventi che permettono di attribuire i Calcari di S'Adde al Batoniano Superiore-Titoniano Inferiore. I dati acquisiti, integrati con quelli provenienti dalla letteratura, permettono di revisionare la cronostratigrafia dei Calcari di S'Adde e di proporne la formalizzazione.

Sulla base dei dati acquisiti, si sono ricostruiti i tassi qualitativi di produzione/esportazione di carbonato: gli intervalli Bathoniano Superiore-Calloviano e Oxfordiano furono periodi di forte riduzione della produzione ed esportazione di carbonato, in accordo con quanto registrato dal margine passivo sud Europeo, caratterizzato da diffusi fenomeni di condensazione.

Per la porzione settentrionale del M.te Albo è stato possibile ricostruire una paleogeografia basin-and-swell ascrivibile al Giurassico Medio, connessa ad attività tettonica regionale di tipo tensionale. Il confronto tra i dati acquisiti e quelli disponibili in letteratura permette d'inserire l'evoluzione locale (M.te Albo) e della Sardegna Orientale nel contesto geodinamico e paleogeografico più ampio del margine passivo sud Europeo.

Introduction

The Corsica-Sardinia microplate belonged to the Jurassic southern European passive margin (Fig. 1) (Fourcade et al. 1993; Dercourt et al. 2000) that represented an intermediate domain between the epicontinental European carbonate platforms (Masse & Alleman 1982; Monleau 1986; Aurell et al. 2003; Rameil 2005; Colombié & Rameil 2007) and the Tethys Ocean with deep basins, drowned carbonate highs and isolated carbonate platforms (Bernoulli & Jenkyns 1974, 2009; Santantonio 1993; Tisljar & Velic 1993; Randisi et al. 2008; Rusciadelli et al. 2009; Erba & Casellato 2010). Due to its paleogeographic position, the Middle to Upper Jurassic carbonate succession of Eastern Sardinia represents a key domain to correlate events between the European and Tethys realms and to understand the Middle-Late Jurassic evolution of the southern European passive margin.

1 Dipartimento di Scienze della Terra "A. Desio", Università degli Studi di Milano, via Mangiagalli 34, 20133 Milano, Italy. E-mail: cristina.casellato@unimi.it; flavio.jadoul@unimi.it
2 Oolithica Geoscience Ltd, 53/57 Rodney Road, Cheltenham GL50 1HX, United Kingdom. E-mail: alessandro@oolithica.net

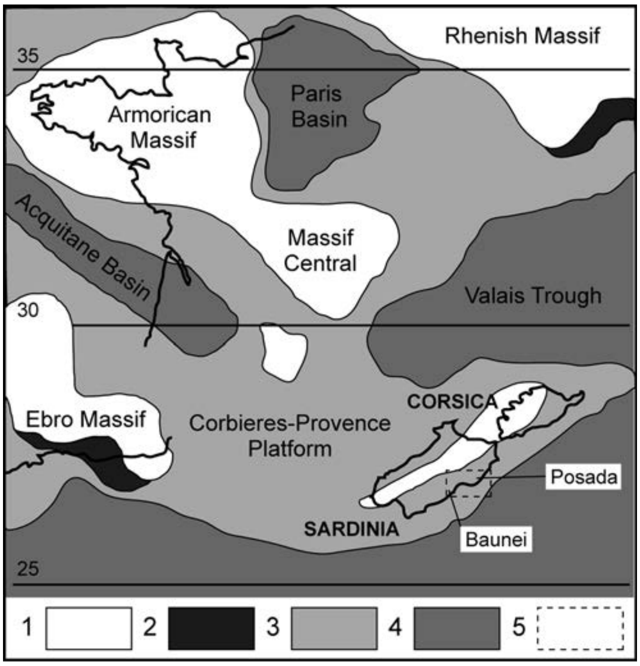

Fig. 1 - Paleogeographic position of the Corsica-Sardinia block in the Late Jurassic. 1) Exposed land; 2) Shallow-water terrigenous environment; 3) Carbonate platforms; 4) Deep basins; 5) Studied area. Modified after Fourcade et al. (1993).

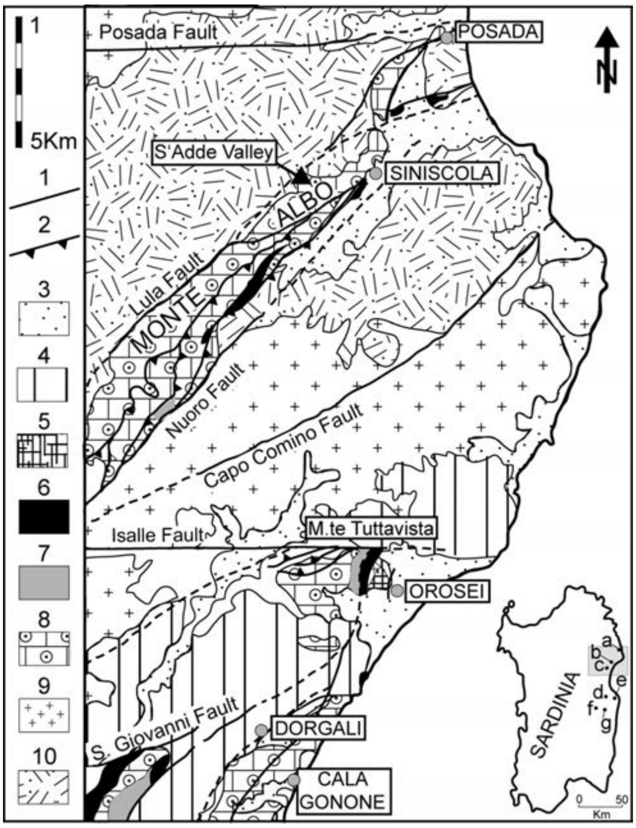

Fig. 2 - Schematic geologic map of the northern half of Orosei Gulf (Posada-Orosei-Cala Gonone). 1) Fault; 2) Thrust fault; 3) Quaternary deposits; 4) Plio-Pleistocene basalts; 5) Orosei conglomerate (Miocene); 6) Cuccuru 'e Flores Conglomerate (Lutetian); 7) Lower Eocene limestone; 8) Jurassic limestone and dolostone; 9) Upper Palaeozoic granitic rocks; 10) Palaeozoic metamorphic rocks. Modified after Dieni et al. (2008). a) Posada, b) Orosei, c) Dorgali, d) Urzulei, e) Baunei, f) Ulassai, g) Jerzu.

In the past decades, several authors studied the Jurassic succession of Eastern Sardinia providing lithostratigraphic and paleogeographic reconstructions (Vardabasso 1959; Amadesi et al. 1961; Calvino et al. 1972; Azéma et al. 1977; Dieni & Massari 1985; Costamagna et al. 2007). Nevertheless, the biostratigraphic ties are scarce and scattered and the entire time framework is poorly constrained especially for the Middle/Late Jurassic boundary and for each age subdivision of Late Jurassic. For this reason, recent regional studies were oriented to detail the bio- and lithostratigraphic framework of the Middle-Upper Jurassic succession of the Orosei Gulf (Jadoul et al. 2007; Lanfranchi 2009; Jadoul et al. 2010). As a part of such studies, this research aims to improve the stratigraphic framework of the Eastern Sardinia carbonate succession at Mt. Albo, which is located north of the Orosei Gulf (Fig. 2). In detail, this study objective is to investigate calcareous nannofossil biostratigraphy of well-exposed sections outcropping in the northern part of Mt. Albo in order to improve the available regional biostratigraphy (ammonite, Dieni et al. 1966) and to constrain the evolution of Middle-Upper Jurassic carbonates in the frame of the southern European passive margin evolution.

Calcareous nannofossils are fossil remains of Coccolithophorids (Lohmann 1902), photoautotrophic algae and primary producers, responsible since the Late Jurassic of biogenic calcareous sedimentation in the oceans. Calcareous nannofossils were widespread in ancient oceans and distributed from coastal areas to open ocean settings, thus they represent the appropriate instrument to investigate the outer ramp/hemipelagic successions of Eastern Sardinia. Calcareous nannofossils can be determined in tight and highly cemented limestone where ammonites, when present, can be hardly isolated and determined. Previous studies have demonstrated the efficacy of this biostratigraphic tool in coeval carbonate succession from Sardinia (Jadoul et al. 2007, 2010).

Stratigraphic setting

The Jurassic succession of Eastern Sardinia (Fig. 2) lies in nonconformity above a Variscan basement of metamorphic and igneous rocks (Vardabasso 1959; Amadesi et al. 1961) and was deposited at a paleolatitude of 20°-25° N (Fourcade et al. 1977). The base of the Jurassic succession consists of Bajocian-Bathonian lenses of continental sandstone and conglomerate of the Genna Selole Formation (Fm.), up to a few metres thick (Dieni et al. 1983; Costamagna & Barca 2004;

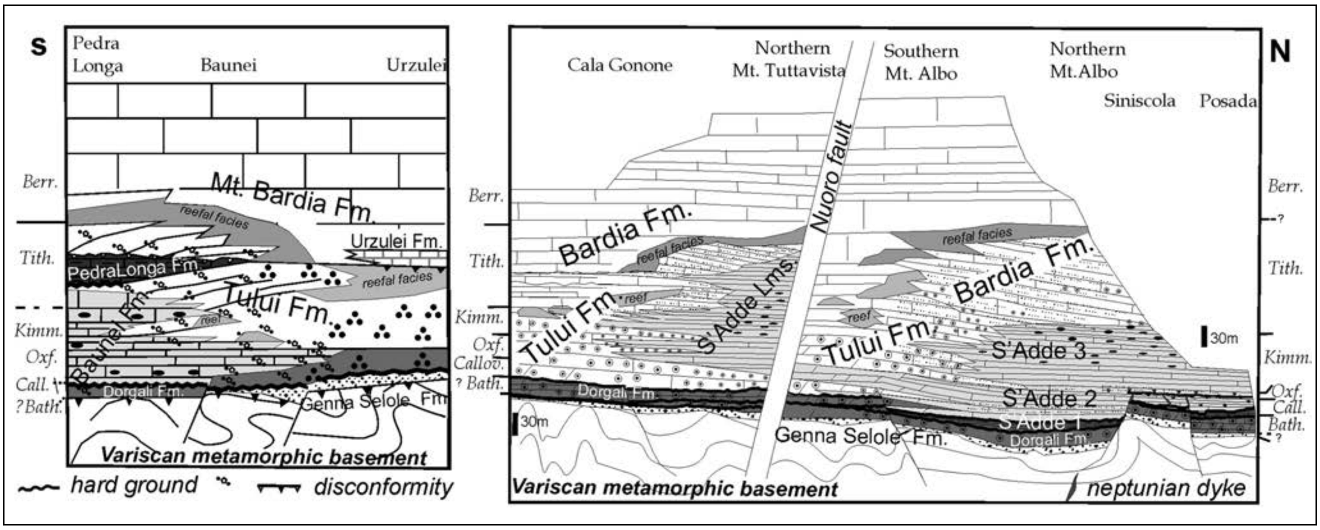

Fig. 3 - Stratigraphic scheme of north (Posada-Siniscola-S'Adde valley-Mt. Tuttavista-Cala Gonone) and south (Pedra Longa-Baunei-Urzulei) Orosei Gulf basins. The scheme regarding the South basin is modified after Jadoul et al. (2010).

Costamagna et al. 2007). The first marine sedimentation, Bathonian in age, consists of carbonate quartz-arenite rapidly evolving to oolitic dolostone (Dorgali Fm.), up to a few tens of metres thick. Thin Fe-rich hardgrounds occur mainly at the top of this formation, suggesting the presence of several hiatuses during the Late Bathonian-Callovian time interval (Dieni et al. 1966). The transition to the overlying shallow-water (Mt. Tului Fm.) and to the outer ramp carbonates is Late Bathonian-Early Callovian in the north portion of Orosei Gulf (S'Adde Lms.), and Late Callovian-Early Oxfordian in the south (Baunei Fm.).

During the Late Jurassic the paleogeographic setting became more diversified. It comprised a carbonate-high (Urzulei-Codula Luna-Codula Sesine), bordered southward (Baunei-Ulassai) and northward (Mt. Albo-Mt. Tuttavista-Cala Gonone) by relatively deep intraplatform basins (Jadoul et al. 2010). The south basin (Fig. 3) recorded the deposition of well-bedded, fine-grained, middle-outer ramp calcilutite of the Baunei Fm. (~100 m thick) that interfingers with shallow-water, thick-bedded oolitic bioclastic calcarenite of Mt. Tului Fm. (Amadesi et al. 1961; S'Adde Lms. – Dieni & Massari 1985; Costamagna et al. 2007; Jadoul et al. 2010). The Mt. Tului-Baunei deposystem is overlain by thin-bedded calcilutite of the Pedra Longa Fm. (upper part of the Lower Tithonian), which are capped by a regional erosional unconformity that represents the downlap surface of prograding clinoforms of Mt. Bardia Fm. (Jadoul et al. 2007, 2010). On the carbonate high, shallow-water limestones of the Mt. Tului Fm. (sensu Jadoul et al. 2010; Mt. Tului Lms. - Dieni & Massari 1985; Genna Silana Fm. - Costamagna et al. 2007) comprise both oolithic shoals and coral-stromatoporoid patch reefs. Peritidal limestones with tepees, lopheritic breccias, black pebbles and charophytes of the Urzulei Fm. divide the shallow-water carbonate of the Tului Fm. from the overlying Mt. Bardia Fm. (Lanfranchi et al. 2008). The progradation of the shallow-water carbonates of Mt. Bardia Fm. is time-transgressive along the Orosei Gulf (Fig. 3): in the south the Mt. Bardia platform progrades during the Late Tithonian on the Pedra Longa Fm. (Lanfranchi et al. 2011, fig. 2), at Mt. Tului and Mt. Albo (this study) it progrades during the Early Tithonian on the S'Adde Lms., at Mt. Tuttavista it progrades during the latest Tithonian-earliest Berriasian (Jadoul et al. 2007).

The studied area is located at the NE edge of Mt. Albo, a 25 km NE-SW elongated carbonate ridge bounded by the Cenozoic strike-slip faults (Isalle, Lula and Nuoro faults, Pasci et al. 1998) (Fig. 2). The carbonate succession of north Mt. Albo is characterized by a continuous unit (up to 180 m thick) of fine-grained calcilutite of the S'Adde Lms. (Dieni & Massari 1985), Callovian to Late Kimmeridgian in age (Dieni et al. 1966).

Studied stratigraphic sections

Three stratigraphic sections have been sampled and studied. They crop out in the area comprised between the S'Adde valley to the south (north Mt. Albo) and Posada to the north (Fig. 2). The studied sections are described below.

a) S'Adde valley section

This section (Fig. 4) was first described by Dieni et al. (1966) and is located in the northern part of the Mt. Albo massif where the Middle to Upper Jurassic limestones are superbly exposed along the left hydrographic slope of the S'Adde valley, from about 700 to

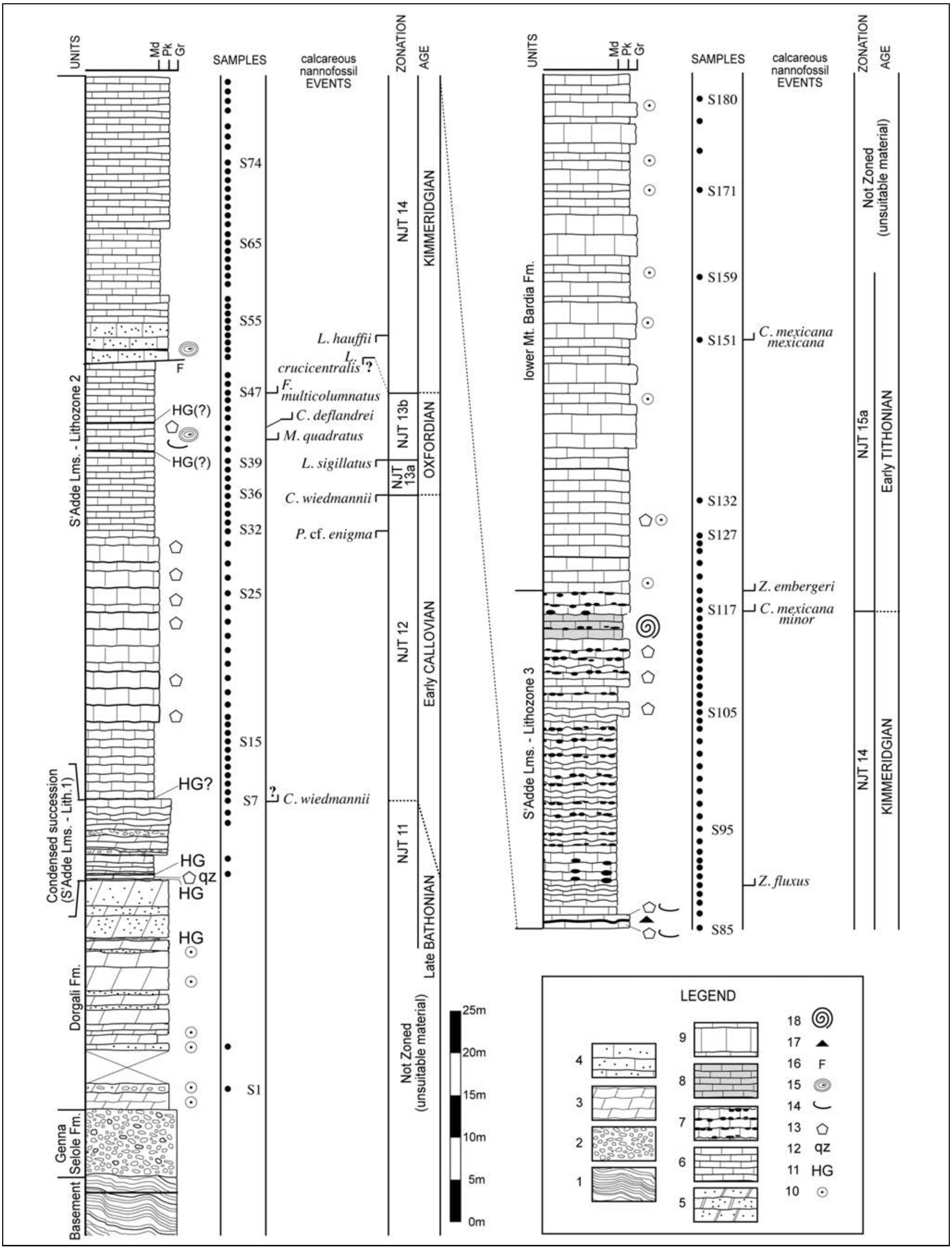

Fig. 4 - The lithostratigraphy and calcareous nannofossil biostratigraphy of S'Adde section. 1) Variscan metamorphic basement; 2) Polygenic conglomerate (Genna Selole Fm.) and fine dolomitic sedimentary breccias (S'Adde Lms. – Lithozone 1); 3) Dolostone; 4) Dolomitic sandstone; 5) Oolitic dolostone; 6) Fine-grained limestone; 7) Limestone with chert nodules; 8) Ammonite-bearing marly limestone; 9) Coarse limestones; 10) Ooids; 11) Hardground; 12) Quartz extraclast; 13) Crinoid; 14) Mollusc; 15) Pelagic oncoid; 16) Fault; 17) Chert; 18) Ammonite fauna belonging to the Beckeri Zone (Dieni et al. 1966).

905 m above see level (from 40° 33' 32" N, 9° 38' 12" E to 40° 33' 30" N, 9° 38' 24" E) (Fig. 5A-B). The studied succession nonconformably overlies a Variscan metamorphic basement of polyphasicly deformed and highly fractured dark grey to greenish micaschist and paragneiss (Carmignani 2001). The topmost part is often red-stained due to high iron content. The studied section has a thickness of more than 200 m and comprises from the bottom to the top the following lithologies (Fig. 4):

– Polygenic, poorly organized, matrix-supported and poorly cemented grey to dark grey conglomerate and sandstone, with prevalent phyllite and quartz pebble to granule. This continental facies can be ascribed to the Genna Selole Formation. Thickness: nearly 8 m.

– Dolomitic fine to medium sand-size quartzarenite, recrystallized dolostone and limestone of the Dorgali Formation. The lowermost part is constituted by dolostone and locally limestone rich in red Fe-stained ooids and quartz extraclasts, passing to well bedded dolostone (grainstone) with pink ooids, then grey dolostone (packstone) with ooids, coated grains and subordinate oncoids, finally dolomitic (fine-grained pack- and grainstone) with ooids, peloids and crinoids. This unit shows a fining and deepening upward trend from coastal hybrid shallow marine environments culminating in open shelf and condensed deposits rich in Fe-oxides/hydroxides and siliciclastic interbeds. Thickness: 25 m.

– Bedded calcilutite and dolomicrite of the S'Adde Limestone. The succession is composed of a lower dolomitic to calcareous lithofacies characterized by marl-silt intercalations and Fe-crusts, followed by bedded limestone with crinoids and at the top limestone with chert nodules. On the basis of these lithofacies three lithozones are recognized as follows:

– Lithozone 1 – Condensed succession. Thin bedded dolostone and peloidal dolomitic limestone with subordinate intercalations of fine-grained micaceous siltstone, dolomitic arenite and marl. Two hardgrounds occur in the lowermost part, and represent the condensed sedimentary succession already described at Posada and Cuile sa Funtana (Fig. 5B) (Dieni et al. 1966). At the top of this lithozone is present a reddish horizon (few metres thick that also outcrops throughout the whole north Mt. Albo) characterized by a network of stratabound cavities with laminated reddish internal fillings. These structures (paleokarst?) might be considered Cenozoic (or even younger) in age. Thickness: 10 m.

– Lithozone 2. The lower part displays light brown to grey mudstone at the base, followed by light brown mudstone and fine peloidal packstone, with crinoids, in 15-40 cm thick beds. The middle part is char-

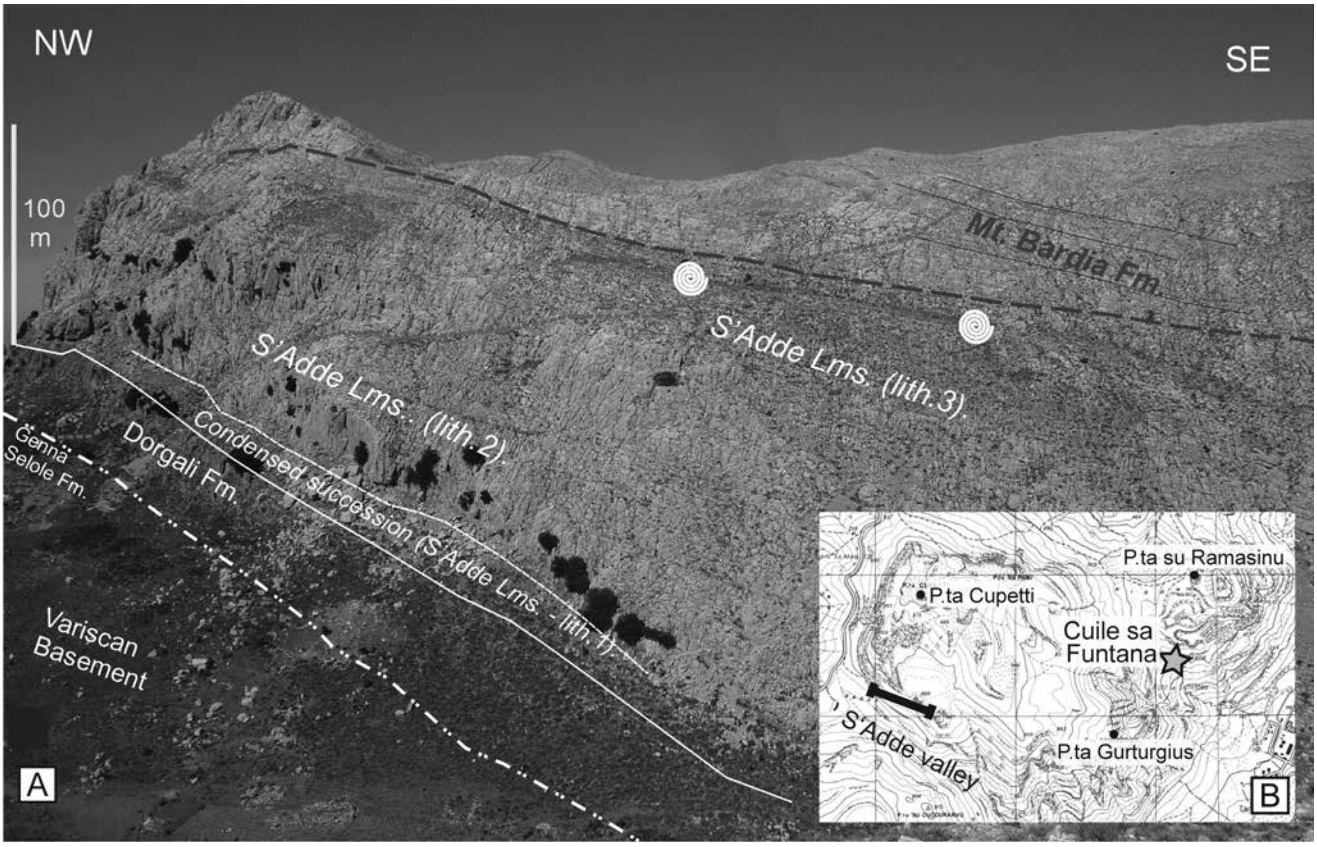

Fig. 5 - A) View of the S'Adde valley with a sketch of the sampled section. B) Extract of topographic map with location of S'Adde valley and Cuile sa Funtana (P.ta Ramasinu).

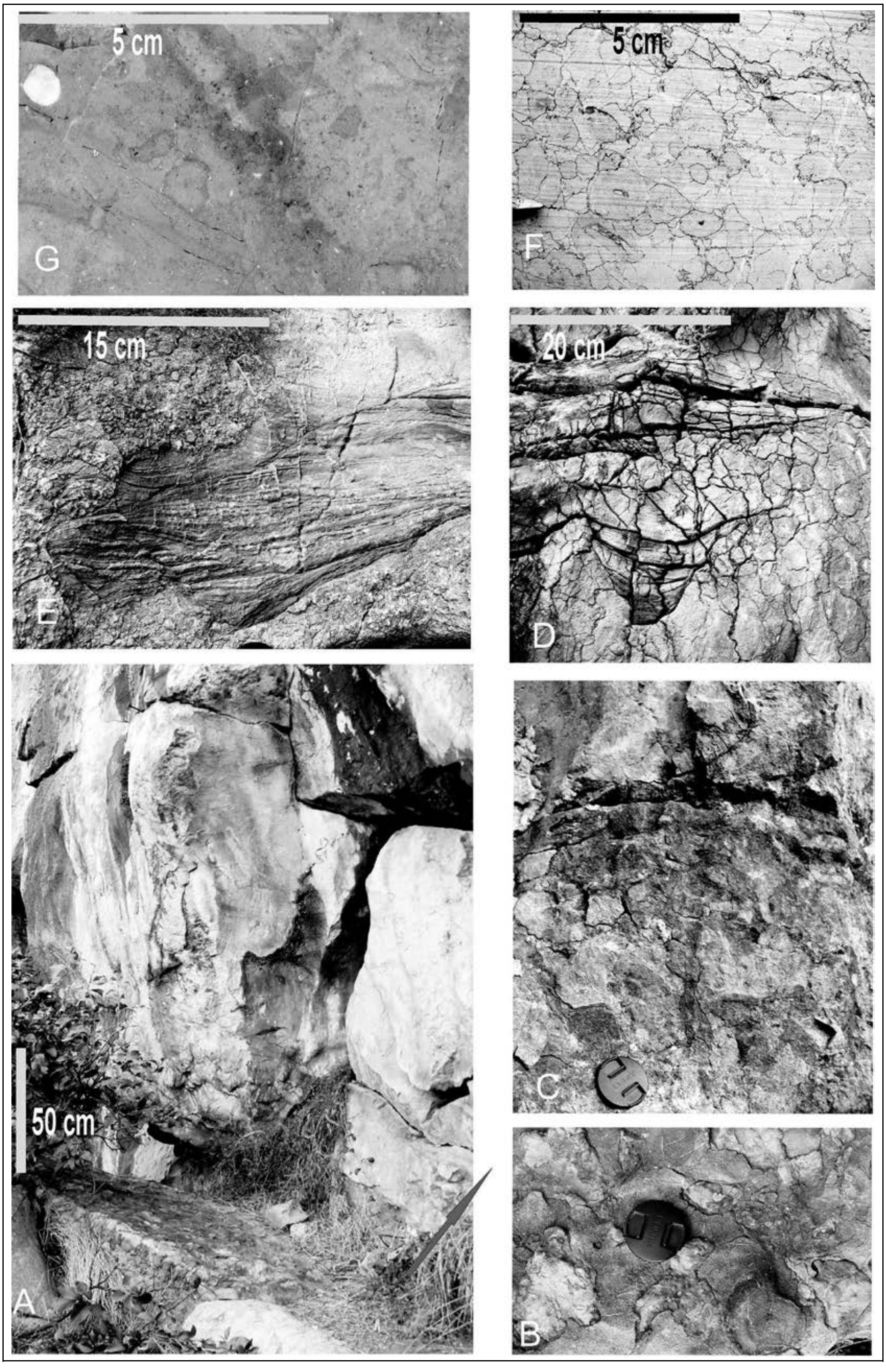

Fig. 6 - Field details of S'Adde Lms. cropping out at Siniscola (Gana 'e Gortoe cave) and S'Adde valley. A) Boundary with Fe-hardground between the oolitic grainstone of Dorgali Fm. and the S'Adde Lms., Lithozone 2, Siniscola; B, C) Detail of the hardgrounds between Dorgali Fm. and S'Adde Lms., Siniscola: B) hardground surface heavily bioturbated and rich in bioclasts, crinoid ossicles, belemnites and ammonoids; C) vertical section; D, E) Detail of the internal laminated sediments in discordant neptunian dykes just at the base of S'Adde succession, Siniscola; F) Stylolitized oncolitic limestones in the lower S'Adde Lms., Lithozone 2. Siniscola abandoned quarry, near Gana 'e Gortoe cave; G) Oxfordian bioturbated intraclastic, oncoidal limestone representing a slow sedimentation interval (sample S50, S'Adde valley section, see Fig. 4).

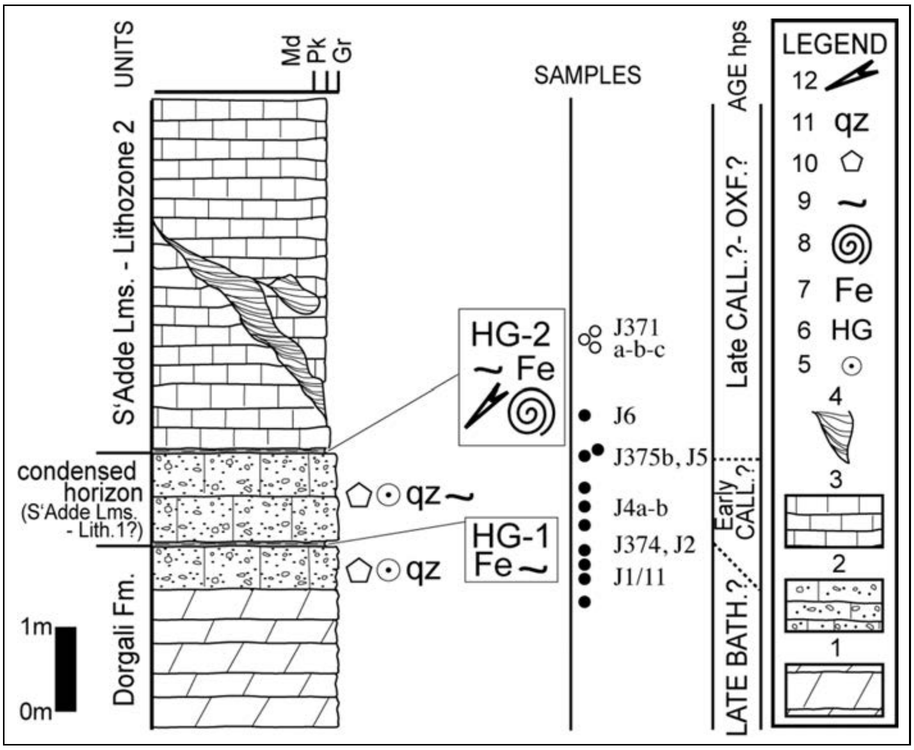

Fig. 7 - The lithostratigraphy of the Siniscola section. 1) Oolitic dolostone; 2) Calcarenite with crinoid ossicles, ooids and quartz-litharenite; 3) Fine-grained limestone; 4) Calcareous laminated sediment infilling the neptunian dykes; 5) Ooid; 6) Hardground; 7) Phosphate; 8) Undetermined ammonoid; 9) Bioturbation; 10) Crinoid; 11) Quartz extraclast; 12) Belemnite. Empty circles indicate samples from fracture internal sediments, analysed in this study for calcareous nannofossil content.

acterized by a ~3 m thick interval bounded by faint stylolitized hardgrounds and constituted by light brown bioturbated mud- and wackestone and intraclastic packstone with centimetre-sized pelagic oncoids (Fig. 6F-G), molluscs shell and crinoids. The upper part of this lithozone consists of dominant whitish grey mudstone to wackestone organized into 30-70 cm thick beds. Thickness: 87 m circa.

– Lithozone 3. Light brown mudstone-fine packstone at the base, followed by ~2 m thick interval of light pinkish fine packstone/wackestone with molluscs and crinoids and displaying cherty bands at the strata interbeds. The main part of this lithozone is constituted by light brown, locally light pink at the bed surface, mudstone-wackestone with brown chert nodules, followed by light brown fine packstone with sparse crinoids and chert nodules. The uppermost part is characterized by a level (~2-3 m thick) of light brown to yellowish calcilutite with marly limestone intercalations, organized into 30-40 cm thick strata, bearing ammonites, aptychi, belemnites, echinoderms and molluscs (for more biostratigraphic detail see Dieni et al. 1966). The overlying last chert horizon marks the boundary with the Mt. Bardia Formation. Thickness: 40 m.

– Lower Mt. Bardia Fm. (sensu Dieni & Massari 1985). Light brown fine-grained peloidal packstone with crinoids, upward intercalated with bioclastic oolitic crinoidal packstone to grainstone in amalgamated metre-thick beds. These lithofacies association is attributed to a middle-ramp progadational system, mainly below wave-base action, as suggested by the lack of current sedimentary structures, low angle clinostratified fine-grained calcarenite and is overlain by coral reef facies of inner-ramp environment. Thickness: more than 65 m.

b) Siniscola outcrop

The condensed section outcropping at Siniscola (Figs. 6A, 7) is located near the entrance of the Gana 'e Gortoe cave (at 40° 34' 40.52" N, 9° 41' 37.61" E)(Fig. 2) and has been firstly described and sampled for this study. The sampled portion of the section has a thickness of a few metres, and is characterized from the bottom by:

– Less than 5 m (boundary with the Variscan basement not cropping out) of recrystallized dolostone, organized into amalgamated metre-thick beds, and characterized at the top by peloidal bioclastic packstone rich in pelagic bivalves (*Bositra*), planktonic foraminifera (*Globuligerina*), benthic Nodosaridae, crinoids, echinoids and scattered ferrigenous ooids with phosphates and Fe-oxides/hydroxides just below the HG-1 (Fig. 8C-D). This facies is also characterized by small neptunian dykes and represents the drowning of the carbonate platform of the Dorgali Fm.

– Condensed horizon (S'Adde Lms. - Lithozone 1) of 1m thick, characterized by Fe-hardgrounds both at its top and bottom. The lower hardground (HG-1) displays at the base abundant and concentrated quartz extraclasts associated with Fe-oxides/hydroxides and phosphatic crusts (Fig. 8A-B). Pelagic bivalves (*Bositra*), planktonic and benthic (Fig 8C-D) foraminifera, ostracodes, serpulids, and crinoid plates are also present. The intermediate level is constituted by coarse bio- and litho-clastic calcarenite, rich in quartz extraclasts, frag-

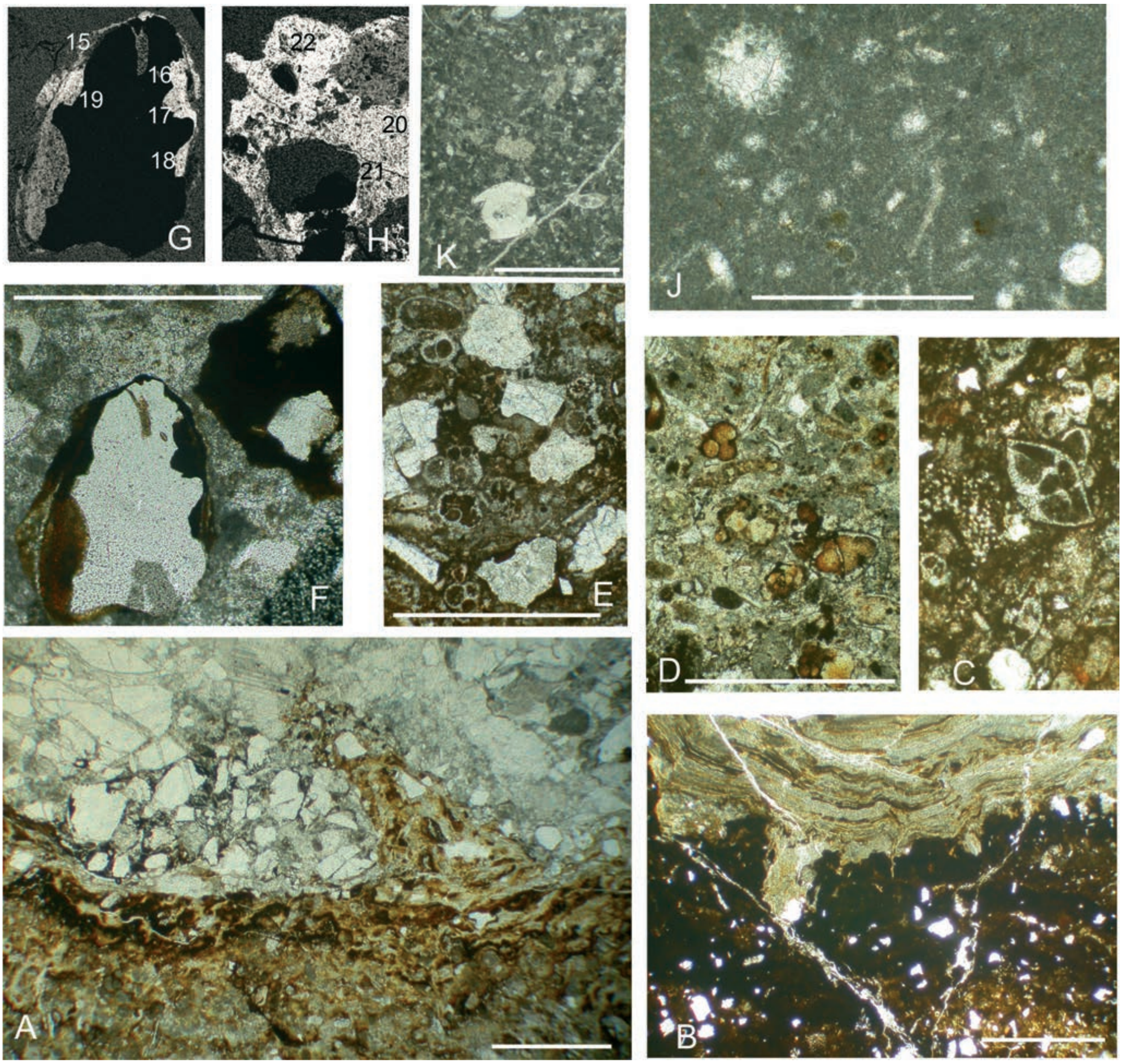

Fig. 8 - Microfacies of Late Bathonian-Callovian condensed interval cropping out at Siniscola (Gana 'e Gortoe cave). A) Boundary between Fe-hardground (HG-1) and intraclastic packstone rich in quartz extraclasts. Below the hardground it is present a pelagic packstone with peloids and intraclasts; B) Detail of the HG-1 with phosphatic and Fe-oxides crust; C, D) Bioclastic peloidal packstone rich in protoglobuligerinids, lagenids often with phosphatic filling (HG-1); E) Bioclastic packstone rich in protoglobuligerinids and quartz extraclast (HG-2); F) Fe-coated quartz extraclast (Polarizing Optical Microscope transmitted light); G, H) Backscattering SEM image of quartz extraclasts analized at the SEM-EDS: numbers represent the selected points analysed; black area are constituted by unaltered quartz, white bands represent Fe-oxide/hydroxide coating. Semiquantitative analyses are reported in Appendix 1; J) Fine-grained wacke- and mudstone with calcitized radiolarians, planktonic foraminifera, sponge spicules (below HG-2). K) Peloidal bioclastic packstone with lagenid foraminifers, echinoids and crinoid fragments (base of S'Adde lithozone 2).

ments of Fe-oxides, Fe-silicate, plagioclase, K-feldspar and metamorphic rock extraclasts, pelagic bivalves (*Bositra*), radiolarians and intraclasts. The upper hardground (HG-2) (Fig. 6B-C, 8E-F-G-H; see also Appendix 1) is similar to the HG-1, but richer in ammonites, belemnites, coarse crinoid fragments, fine benthic foraminifera and reworked ooids.

– S'Adde Lms. - Lithozone 2. The base is characterized by fine-grained packstone with peloids, foraminifera, ostracodes, crinoids and reworked Fe-oxides and phosphatic fragments (Fig. 8J-K). The base of the S'Adde Lms. here displays a strong stylolitization and a developed open fracture network, infilled with laminated sediments characterized at the base by polychrome (greenish and reddish) marls, then passing to grey calcilutite, similar to the host rock, and grey to reddish calcarenite with intraclasts and echinoids (Fig. 6D-E).

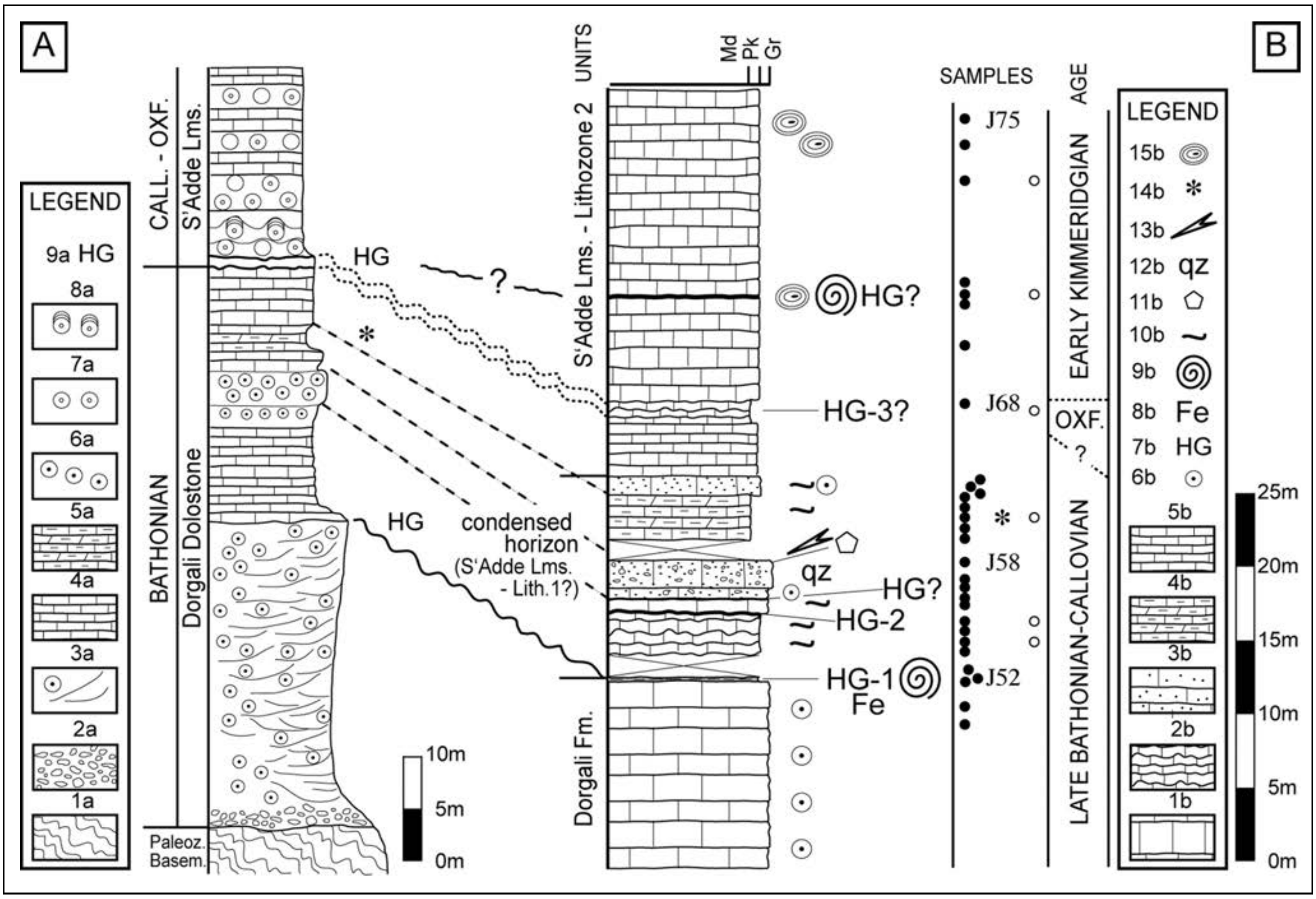

Fig. 9 - A) The lithostratigraphy of Posada section described by previous authors (Massari & Dieni 1983). 1a) Metamorphites; 2a) Quartzose conglomerate and sandstone; 3a) Cross-bedded oolitic limestone and dolostone; 4a) Outer shelf limestone and dolostone; 5a) Outer shelf marls; 6a) Oolitic dolostone; 7a) Oncolitic limestone; 8a) Domical stromatolites developed on oncoids; 9a) Hardground.
B) The lithostratigraphy of Posada section described in this study. 1b) Oolitic calcarenite; 2b) Nodular fine limestone; 3b) Calcarenite with crinoid ossicles, ooids and quartz-litharenite; 4b) Marly limestone; 5b) Calcareous limestone; 6b) Ooids; 7b) Hardground; 8b) Phosphate; 9b) Ammonite (Dieni et al. 1966) and undetermined ammonoid; 10b) Bioturbation; 11b) Crinoid; 12b) Quartz extraclast; 13b) Belemnite; 14b) Sample F.1.c after Dieni & Massari (1985) studied for calcareous nannofossils; 15b) Pelagic oncoids. Empty circle indicates samples analysed in this study for calcareous nannofossil content.

c) Posada section

The Posada section is well known in the literature and has been described in detail for bio- and microfacies (Dieni et al. 1966, fig. 1; Massari & Dieni 1983, fig. 1; Dieni & Massari 1985, fig. 67; Giusberti & Coccioni 2003, fig. 2) (Fig. 9A). The section presented in this study (at 40° 38' 18" N, 9° 43' 24" E) (Fig. 9B) crops out on the northern side of the Posada hill, and is characterized from the base to top as follow:

– Massive amalgamated light grey oolitic grainstone a few tens of metre thick, representing a calcareous lithofacies belonging to the top of Dorgali Formation.

– Condensed horizon (S'Adde Lms. - Lithozone 1) characterized from the bottom by: a) one hardground (HG-1) with Fe-oxides/hydroxides, phosphate and bioturbated packstone; b) well bedded, bioturbated, nodular limestone with silt interbeds capped by a hardground (HG-2) similar to HG-1 (Fig. 10A); c) one 2 m thick bed of bioclastic calcarenite with crinoids, belemnites, abundant angular extraclasts of quartz, feldspars, fragments of hardground and reworked ooids (Fig. 10B); d) ~4 m of thinly bedded marly limestone alternated with dolomitic marl; e) one 1 m thick bed of bioturbated oolitic calcarenite.

– S'Adde Lms. - Lithozone 2. The base is characterized by a 4 m thick horizon of bedded calcarenite, followed by finer-grained calcarenite culminating in a 1 m thick layer of amalgamated nodular calcilutite, possibly bearing faint hardgrounds (HG-3). This level is overlain by whitish grey fine pack- and wackestone, sometimes bearing oncoids and ammonites possibly associated with low sedimentation rate horizons (Fig. 10C).

Methods

A total of 182 samples with a sampling spacing of about 1 metre were collected along the S'Adde valley section (Fig. 4, 5A), 13 and 36 samples were taken from Siniscola (Fig. 7) and Posada (Fig. 9B) sections, respectively. The investigated lithologies for calcareous nannofossil biostratigraphy comprise fine-grained limestone (calcilutite) be-

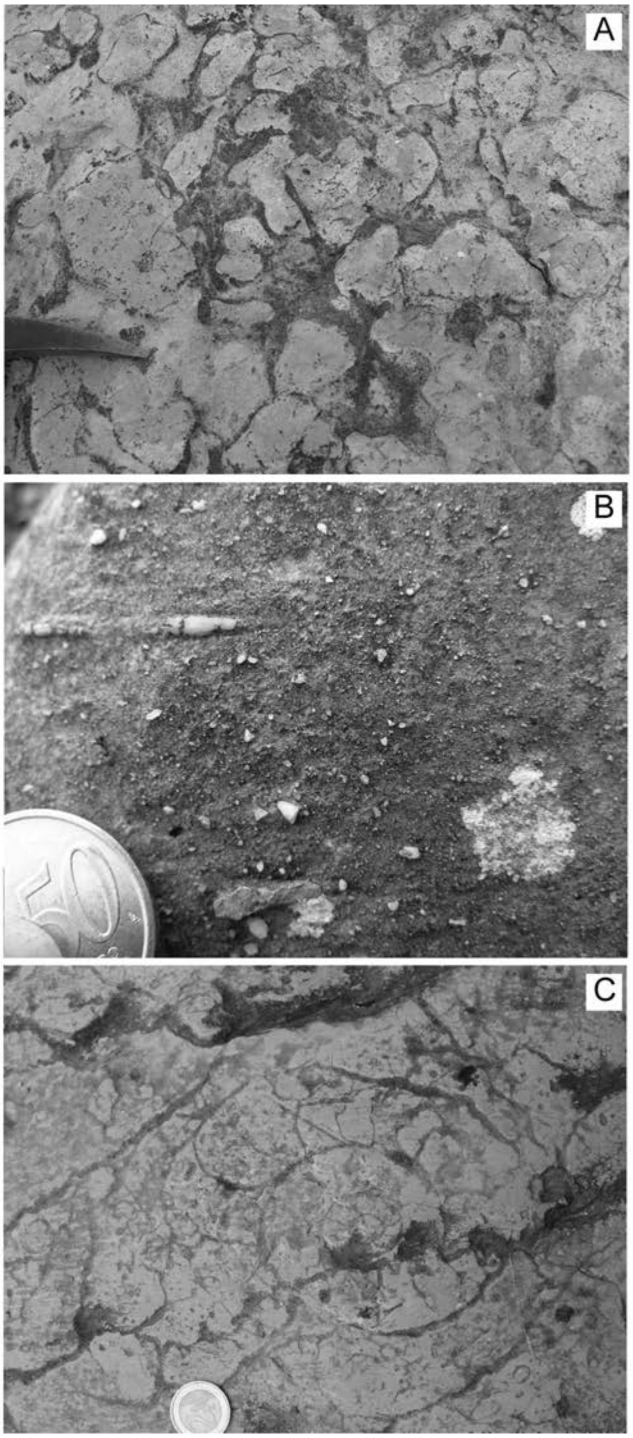

Fig. 10 - Field details of condensed interval of S'Adde Lms. outcropping at Posada section (Fig. 6). A) Detail of the hardground surface between Dorgali and S'Adde Limestone; B) Dolo-litharenite with abundant quartz extraclast, crinoids, ooids, belemnites of S'Adde Lms. – Lithozone 1; C) Undetermined ammonite.

longing to S'Adde Lms. and fine-grained limestone of Mt. Bardia Formation. Biostratigraphic analyses were performed on smear slides prepared as follows: a small amount of rock material was powdered adding few drops of bi-distillate water; the obtained suspension was mounted onto a microscope slide, covered with a slide cover and fixed with Norland Optical Adhesive, without centrifuging, ultrasonic cleaning or settling the sediment in order to retain the original composition. Smear slides were inspected using a light polarizing microscope, at 1250X magnification. The biostratigraphic scheme after Casellato (2010) was adopted. Preservation of calcareous nannofossils was characterized adopting the classes described by Roth (1983): E1 (slight etching); E2 (moderate etching); E3 (strong dissolution); O1 (slight overgrowth); O2 (moderate overgrowth); O3 (strong overgrowth).

Estimate of nannofossil total abundance was recorded as follows: F (few), 1 specimen every 1-10 fields of view; R (rare), 1 specimen every 11-50 fields of view; RR (very rare), 1 specimen every 51-100 fields of view; B (barren), no specimen found.

Two samples (Siniscola section) were studied with a Cambridge 360 scanning electron microscope (SEM) to obtain the elemental composition of the coating surrounding quartz extraclasts. Analyses were performed with an energy dispersive X-ray analysis (EDS Link Isis 300) requiring a carbon-coated thin section. Analysed elements were standardized using several single-element standards (Micro-Analysis Consultants Ltd). Elemental concentrations measured by EDS are reported as oxide weights normalized to 100% (Appendix 1).

Calcareous nannofossil biostratigraphy of S'Adde Limestone

Calcareous nannofossils are very rare to rare along the entire S'Adde valley section: the assemblages recognized are dominated by the genera *Watznaueria* (Pl. I, figs 1-6, 8-9) and *Cyclagelosphaera* (Pl. 1, figs 7, 10, 11-12), that are the most resistant coccoliths to diagenetic modifications (Roth 1986). The investigated interval has very poor nannofossil preservation: often specimens are etched and/or affected by overgrowth. Nevertheless it has been possible to identify some taxa described in the literature and to point out a few primary calcareous nannofossil events, namely 7 first occurrences (FO) as well as 6 last occurrences (LO) (Fig. 4). Therefore, total of 13 calcareous nannofossil bioevents characterizing the lowermost Callovian to Lower Tithonian interval are recognized. The FO of *Cyclagelosphaera wiedmannii* (Pl. 1, fig. 11-12) has been detected at the base of Lithozone 2 (S'Adde Lms.), followed by the LOs of *Pseudoconus enigma* (Pl. 2, fig. 1) and *C. wiedmannii* in the lower middle part of Lithozone 2. Thus this interval might be assigned to the lowest Callovian (Reale & Monechi 1994; Mattioli & Erba 1999; Casellato 2010). The LO of *Lotharingius sigillatus,* shortly followed by the FOs of *Microstaurus quadratus* (Pl. 2, figs. 4-6) and *Cyclagelosphaera deflandrei*, are recognized in the middle part of Lithozone 2

PLATE 1

1) *W. fossacincta*, S24; 2) *W. barnesiae*, S95; 3) *W. barnesiae* S91; 4) *W. britannica*, S26, central bridge is lacking probably due to dissolution; 5) *W. britannica*, S85, central bridge is lacking probably due to dissolution; 6) *W. manivitiae*, S6; 7) *C. margerelii* (and a *W. manivitiae* sideways), S109; 8) *W. manivitiae* large, S49; 9) *W. manivitiae*, S85; 10) *C. margerelii*, S96; 11) *C. wiedmannii*, S24; 12) *C. wiedmannii*, S32, the rim displays evident overgrowth.
Scale bar represents 5 μm.

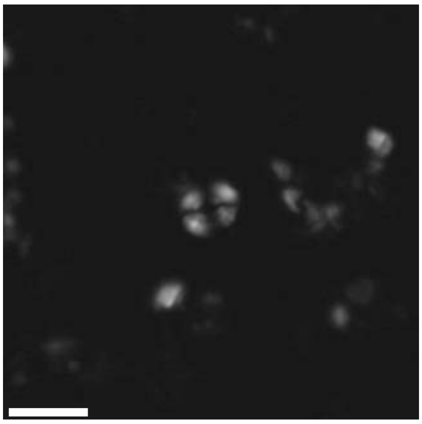

1 - *W. fossacincta*

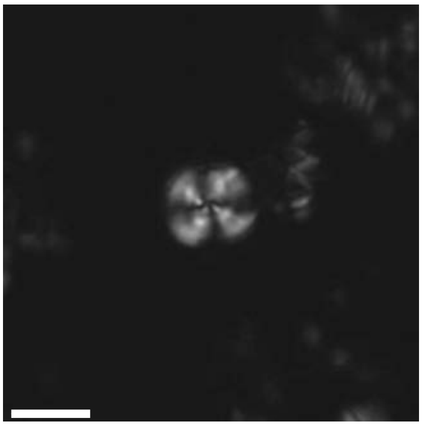

2 - *W. barnesiae*

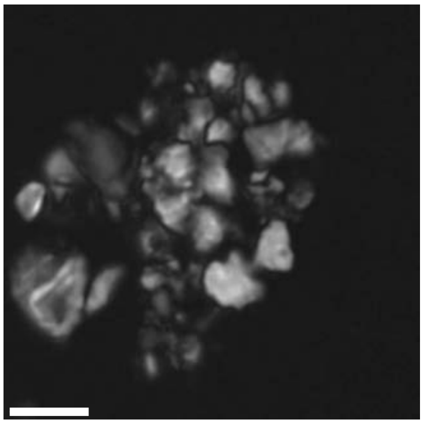

3 - *W. barnesiae*

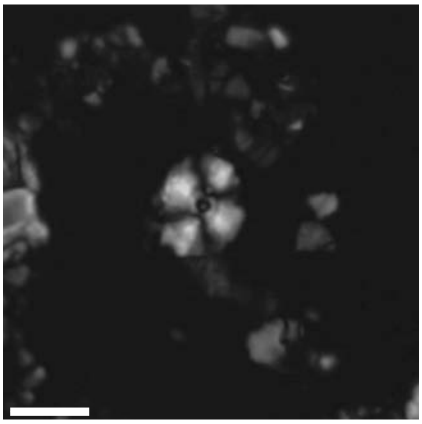

4 - *W. britannica*

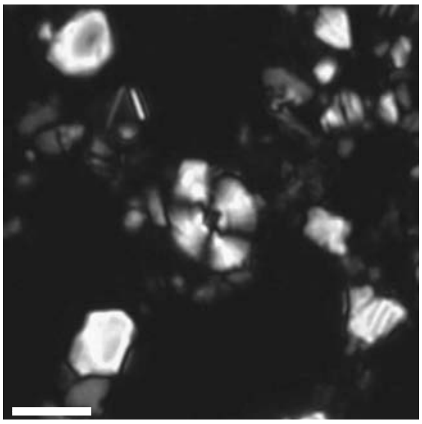

5 - *W. britannica*

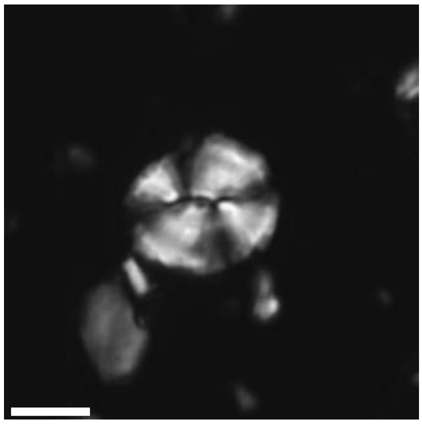

6 - *W. manivitiae*

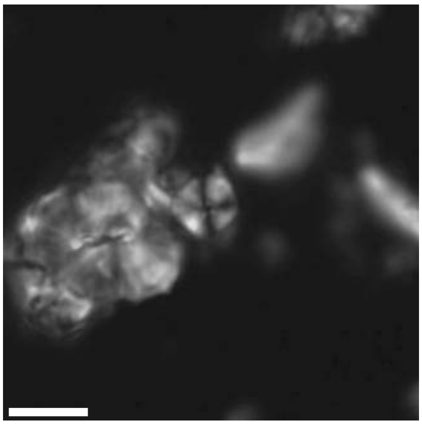

7 - *C. margerelii*

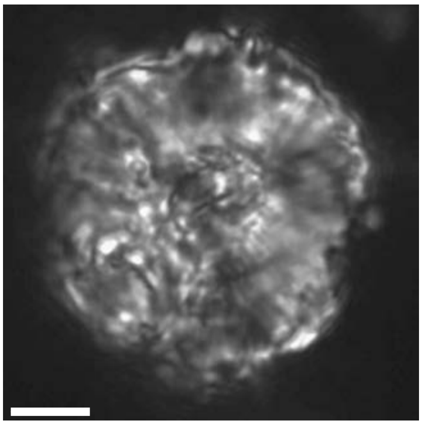

8 - *W. manivitiae* large

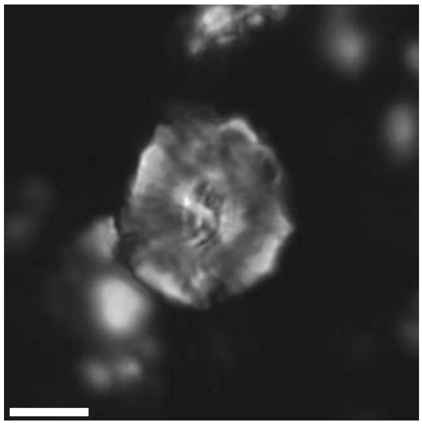

9 - *W. manivitiae*

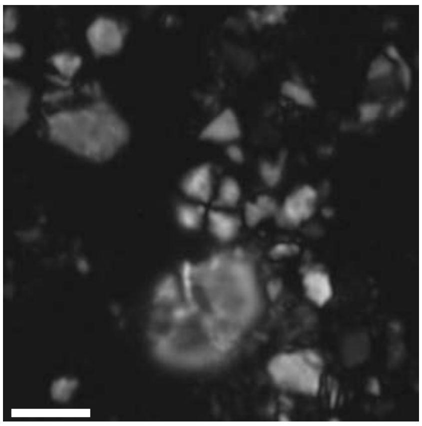

10 - *C. margerelii*

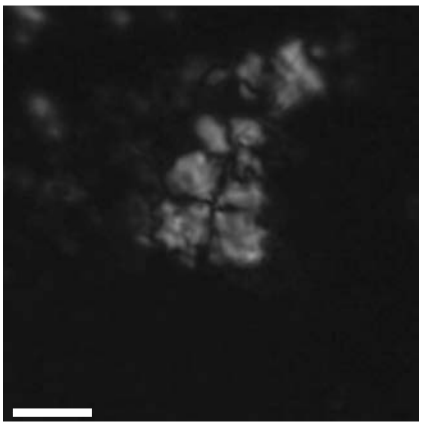

11 - *C. wiedmannii*

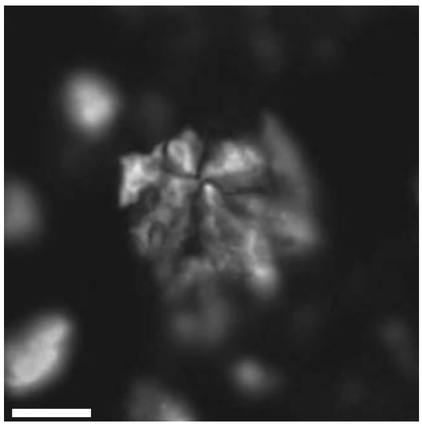

12 - *C. wiedmannii*

(S'Adde Lms.). The FO of *Faviconus multicolumnatus* (Pl. 2, figs. 7-8), detected slightly above indicates a latest Oxfordian-earliest Kimmeridgian age. Therefore these events together permit to assign this condensed interval to the Oxfordian. The FO of *Conusphaera mexicana minor* (Pl. 2, fig. 9) lies at the top of Lithozone 3 (S'Adde Lms.), a few metres below the S'Adde Lms./ Mt. Bardia Fm. boundary, and might permit to approximate the boundary to lowest Tithonian. This event lies slightly above the bio-horizon described by Dieni et al. (1966), that yielded an ammonite fauna certainly belonging to the Beckeri ammonite Zone (latest Kimmeridgian). The FO of *C. mexicana mexicana* is the very last event detected in the studied section, and lies within the Mt. Bardia Fm., dating to the Early Tithonian the lowest part of this formation (sensu Dieni & Massari 1985) in the Mt. Albo massif. Thereafter, carbonate deposits are constituted by unsuitable material for the calcareous nannofossil investigations: indeed the Mt. Bardia Fm. yielded a very rare to barren nannofloral association.

Range chart of calcareous nannofossils of the S'Adde valley section is given in Appendix 2. A list of species recognized is reported in Appendix 3.

The carbonate sediments infilling the paleofracture outcropping in the Siniscola village (Fig. 7, 6D-E) were also sampled for calcareous nannofossil investigations. Three samples were analysed, two of them resulting barren, while one giving a nannofloral association characterized only by well-preserved Mesozoic coccoliths of genus *Watznaueria*, useless to asses a more precise age attribution.

Calcareous nannofossil investigations at the Posada section (Fig. 9B) have been already performed on a marly layer by F. Proto Decima (in Dieni & Massari 1985), but nannofossil content was useless for any age assignment. In this study further six samples have been analysed: although calcareous nannofossils are rare and poorly preserved, it has been possible to recognize an association useful to detail age assignment. In particular the presence of *F. multicolumnatus* and *C. deflandrei*, along with the absence of *C. mexicana minor*, permits to frame the lowermost part of the Lithozone 2 at Posada in the Late Oxfordian time interval.

Discussion

Litho- and chronostratigraphy of S'Adde Limestone

The hardgrounds that stand at the base of the S'Adde Lms. can be attributed to the Late Bathonian-Callovian according to ammonite association (Dieni et al. 1966; Dieni & Massari 1985; Dieni & Radoičić 1999), thus the overlying calcilutites have been attributed to the Oxfordian and the Kimmeridgian. Previous studies (Massari & Dieni 1983; Dieni & Massari 1985, fig. 17-18) adopted a boreal chronostratigraphic scale, here it is preferred the Mediterranean one, as the succession yielded a Mediterranean fauna and belongs to the Tethyan Domain. The chronostratigraphy of the Middle-Upper Jurassic succession of Mt. Albo area is here refined on the basis of calcareous nannofossil data integrated with previous age assignments. Calcareous nannofossils indicate that the S'Adde Lms. (S'Adde valley section) spans the latest Bathonian to Early Tithonian time interval, in agreement with previous authors. The Lithozone 1 described at S'Adde valley (Fig. 4) correlates with the condensed horizon at Siniscola (Fig. 7) and Posada (Fig. 9B). This lithozone was previously included in the upper Dorgali Fm. on the basis of dolomitization, but as it displays a deepening upward trend (typical sequence of platform drowning), it is here considered as a transitional unit genetically bounded to the S'Adde Limestone (Tab. 1). Its age might be latest Bathonian to earliest Callovian at S'Adde valley (Fig. 4) and possibly at Posada (Fig. 9B), whilst no precise age can be inferred for Siniscola as this lithozone is reduced to 1 m thick condensed horizon with Fe- and phosphatic hardgrounds (Figs 7, 6A-B-C). At Cuile sa Funtana it comprises all the Callovian (Dieni et al. 1966). On the basis of calcareous nannofossil assemblages, the Lithozone 2 spans the Early Callovian to possibly the Early Kimmeridgian: it is well developed and expanded at S'Adde valley, while it is definitely more condensed at Posada (Figs 4, 9B). In particular the Oxfordian time interval, previously inferred to be extremely condensed or even absent (Dieni et al. 1966), has been identified in the S'Adde valley where it is represented by about 13 m thick interval characterized by low sedimentation rate horizons and faint hardgrounds (Fig. 4). The Lithozone 3 in S'Adde valley section spans the Late Kimmeridgian-earliest Tithonian time interval.

Qualitative sedimentation rates and their implications

Achieved chronostratigraphy permits to deduce some considerations about average sedimentation rates of the S'Adde Limestone: the Upper Bathonian-Callovian and the Oxfordian are intervals characterized by the lowest values of sedimentation rate (~2-5 m/My), while the Kimmeridgian and the Lower Tithonian yielded an average rate of about 15 m/My. The lowest values are plausibly a consequence of a few hardgrounds testifying for important hiatuses. Upper Bathonian-Callovian hardgrounds are rich in iron, phosphate and siliciclastic grains (angular quartz, K-feldspar, plagioclase) suggesting a strong reduction of carbonate production/ sedimentation. Two causes are invoked for these sedimentation rates: 1) a renewed erosion of subaerially exposed metamorphic and volcanic rocks, 2) a submarine exhumation of basement rocks in correspondence of listric faults. Both cases are framed within a rifting tectonic activity, linked with the opening of the Alpine

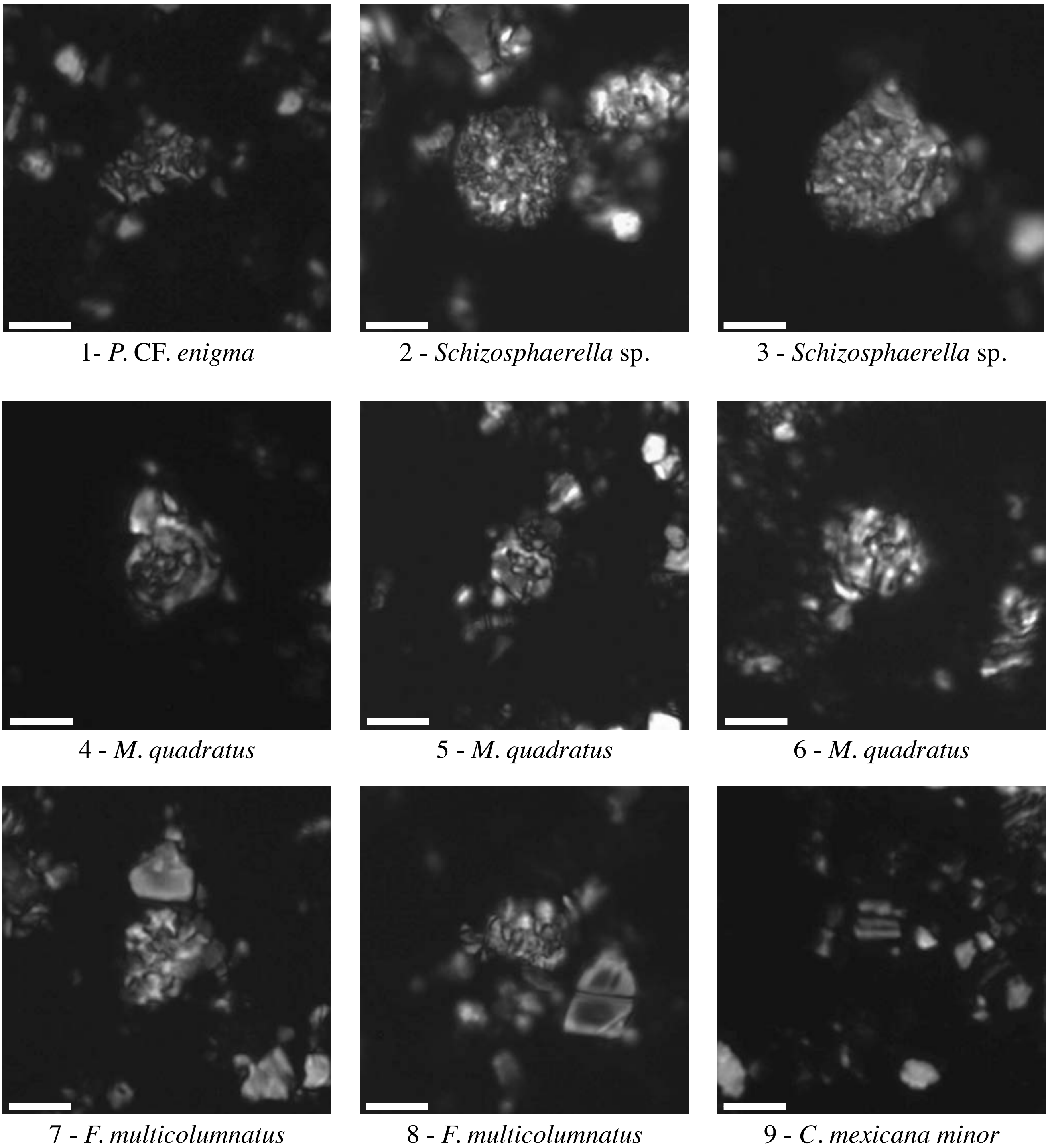

PLATE 2

1) *P.* cf. *enigma*, S26; 2) *Schizosphaerella* sp., S57; 3) *Schizosphaerella* sp., S91; 4) *M. quadratus*, S74; 5) *M. quadratus*, S57; 6) *M. quadratus* (and a fragment of *Faviconus* on lower right), S52; 7) *F. multicolumnatus* (fragment), S91; 8) *F. multicolumnatus* (fragment), S85; 9) *C. mexicana minor*, S121. Scale bar represents 5 µm.

Tethys and the Atlantic oceans. The Oxfordian hardgrounds are exclusively calcareous, less developed than the older ones, and are often strongly bioturbated, pseudo-nodular in aspect and locally rich in pelagic oncoids (Massari & Dieni 1983)(Pl. III, fig. F). They can be interpreted as a consequence of a decrease in the production/exportation of carbonate mud from the adjacent platform, and the decrease of carbonate shedding can be related to a relative sea-level fall (highstand shedding – Schlager et al. 1994). Along the S'Adde valley, the Oxfordian succession shows very poorly developed hardgrounds suggesting that this area likely represented the depocentre of the basin. On the contrary at Posada and around Siniscola the hardgrounds are better devel-

S'Adde section	Lithology	Thickness	Environmental interpretation	Lithostratigraphy (previous authors)	Lithostratigraphy (this study)	Age
Dorgali Fm.	Dolomitic fine to medium quartz-arenite, Fe-stained ooids & coated grain dolomitic grainstone in metre thick, often amalgamated beds.	25m	Coastal high-energy shoal, locally lagoon and beach	Dorgali Dolostone	Dorgali Fm.	Late Bathonian
Condensed succession (S'Adde - Lithozone 1)	Dolomitic mudstone and peloidal wacke-packstone with dolomitic marly dolostone, rare silty sandstone interbeds. HG are both present at the base and at the top of the unit.	10m	Middle-outer ramp with low sedimentation rate	Dorgali Dolostone	S'Adde Lms.	Late Bathonian\ Early Callovian
S'Adde - Lithozone 2	Mudstone to crinoid-micropeloidal wacke-packstone, rare fine grained peloidal, oo-bioclastic grainstone intercalations. Thickening up trend (15-40 cm to 30-70 cm at the top).	87m	Mainly outer ramp/ intraplatformal basin	S'Adde Lms.	S'Adde Lms.	Upper Callovian to (Early) Kimmeridgian
S'Adde - Lithozone 3	Mudstone, wackestone and peloidal bioclastic packstone with chert nodules locally ammonites. 30 to 50 cm beds, l cm-thick marly interbeds at the top.	40m	outer ramp/ intraplatformal basin	S'Adde Lms.	S'Adde Lms.	(Late) Kimmeridgian to earliest Tithonian
Mt. Bardia Fm.	Peloidal-crinoid packstone to oo-bioclastic grainstone in m-thick beds, often amalgamated locally low angle clinostratified.	65m (top missing)	Mainly middle ramp/slope	Mt. Bardia Fm.	Mt. Bardia Fm.	Early Tithonian

Siniscola section	Lithology	Thickness	Environmental interpretation	Lithostratigraphy (previous authors)	Lithostratigraphy (this study)	Age
Uppermost Dorgali Fm.	Bio-intraclastic, peloidal packstone with open marine benthic\planktonic microfacies.	1m (base missing)	Open subtidal, drowning of the Dorgali platform	Dorgali Dolostone	Dorgali Fm.	Late Bathonian ?
Condensed succession (S'Adde - Lithozone 1)	Fe-hardgrounds, bio-lithoclastic packstone, with qz extraclasts and Fe-oxides, phosphates.	1m	carbonate swell, condensed sedimentation	Dorgali Dolostone	S'Adde Lms.	Early Callovian ?
S'Adde - lowermost Lithozone 2	Bio-intraclastic, peloidal packstone, wackestone with open marine benthic\planktonic microfacies. Neptunian dykes.	4\5m	carbonate swell, low sedimentation rate	S'Adde Limestone	S'Adde Lms.	Late Callovian ?

Posada section	Lithology	Thickness	Environmental interpretation	Lithostratigraphy (previous authors)	Lithostratigraphy (this study)	Age
Uppermost Dorgali Fm.	Oolitic grainstone, Fe-stained at the top.	5m	Oolitic shoals	Dorgali Dolostone	Dorgali Fm.	Bathonian
Condensed succession (S'Adde - Lithozone 1)	Fe-hardgrounds, bio-lithoclastic bioturbated packstones\rudstone with qz extraclasts and Fe-oxides.	about 13 m	carbonate swell, condensed sedimentation	Dorgali Dolostone	S'Adde Lms.	Late Bathonian-Callovian
S'Adde - Lithozone 2	Nodular bio-intraclastic, peloidal packstone, wackestone with open marine benthic\planktonic microfacies, local pelagic oncoid and ammonoids.	25m (top missing)	middle-outer ramp, low sedimentation rate	S'Adde Lms.	S'Adde Lms.	Oxfordian-Kimmeridgian

Tab. 1 - Synthesis of S'Adde Lms. lithofacies associations.

oped (see Dieni et al. 1966 for further details) suggesting that these sites were located on a swell. Coeval Upper Bathonian-Callovian and Oxfordian succession from the south European margin display a similar reduction of sediment production during these times. Submarine hiatuses and Fe-hardgrounds around the Late Bathonian-Callovian time interval are reported from Iberian carbonate platform (Ramajo & Aurell 2008), Portugal (Azerêdo et al. 2002), Hungary (Tisza terrane, Vörös 2011), Alpine Tethys (Calabria – Santantonio & Teale 1985), and Himalaya (Garzanti et al. 1989), and mirror a serious restriction of the carbonate budget, possibly due to sudden cooling and global sea-level fall (Dromart et al. 2003). Condensed horizons (with pelagic oncoids, sensu Massari & Dieni 1983) as well as demise of carbonate production during the Oxfordian are reported from the Iberian carbonate platforms (Gómez & Fernández-López 2006; Reolid et al. 2010), Jura Mountains (Padden et al. 2001; Védrine & Strasser 2009; Louis-Schmid et al. 2007), Paris Basin (Corbin et al. 2000; Carpentier et al. 2010), and Hungary (Tisza terrane, Vörös 2011). All these examples are framed in a time of changes in carbonate sedimentation probably linked to significant perturbations of the marine carbon reservoir (Jenkyns et al. 2002; Weissert & Erba 2004) and climate changes (Abbink et al. 2001).

The Kimmeridgian-Early Tithonian high average sedimentation rates could reflect abundant production and exportation of carbonate mud from shallow-water factories (Mt. Tului Fm.) toward the basin (S'Adde Lms.). The abundant chert nodules of Lithozone 3 are considered as a useful regional marker for the Upper Kimmeridgian interval as they have been observed also in the southern basin (Jadoul et al. 2009, 2010). The abundance of chert nodules might reflect the latest Jurassic colonization of siliceous sponges, associated with coral-sponge-microbialite reefs documented for Eastern Sardinia (Ricci et al. 2012). The higher sedimentation rates of S'Adde basin might correlate with the supra-regional increase of carbonate productivity (shallow and pelagic) of both European shallow-water platform and Tethys Ocean (Roth 1989; Weissert & Erba 2004).

S'Adde area paleogeographic reconstruction

The carbonate sediments infilling the cavity network at Siniscola (Fig. 7) have been interpreted as neptunian dykes (Fig. 6D-E). Some of these structures show features resembling paleokarst cavities filled by internal sediments. However, as the sediments infilled are marine and pelagic in nature, on the basis of calcareous nannofossil content, and reworked Fe-hardgrounds are present, the interpretation as neptunian dyke is more reasonable. This fracture network, locally oriented NW-SE and N-S, may be presumably Late Callovian or Oxfordian in age, as it cuts the lowermost part Lithozone 2 and is infilled by sediments resembling the ones characterizing the rest of Lithozone 2. The development of neptunian dykes might be linked to a synsedimentary rifting activity. Tectonic movements have plausibly contributed to delineate, in the Orosei Gulf area, a Middle Jurassic basin-and-swell setting, bounded by small scale normal faults, which contributed to the higher subsidence and/or sedimentation rates of the basin depocentre S'Adde Lms. (and Baunei Fm.), as well as partially favouring condensation on the Callovian Posada-Siniscola-Cuile sa Funtana swells. The depocentre of the Upper Jurassic basin, as suggested by the maximum thickness of the S'Adde Lms. and by the progradational trends of the overlying lower Mt. Bardia Fm. carbonate, was possibly located in the Siniscola area structural high. The Mt. Tuttavista succession could represent a coeval (sub-)basin, developed on the southern side of the Posada-Siniscola-Cuile sa Funtana ridge, maybe lasting until the Late Tithonian (Jadoul et al. 2007) (Fig. 3). The S'Adde Lms. outcropping at Cala Gonone (Mts. Tului and Bardia) possibly represents a marginal portion of the Mt. Tuttavista basin (Fig. 3).

Comparison with the Orosei Gulf succession

The southern portion of Orosei Gulf still lacks a precise chronostratigraphy of the uppermost Dorgali – Baunei Fm./S'Adde Lms. interval. Nevertheless, it is worth noting the presence of some Fe-hardgrounds/firmgrounds and dolomitized pelagic limestone of different thickness outcropping in the Genna Selole-Baunei-Jerzu areas, possibly representing a southern equivalent of the Upper Bathonian-Oxfordian basin-and-swell system of north Mt. Albo. Moreover, the Kimmeridgian pelagic carbonates with chert of the upper Baunei Fm. are similar to the Lithozone 3 of the S'Adde Lms. (Fig. 3).

The Kimmeridgian-Tithonian interval displays a more complex evolution in the south: a shallow-water carbonate system with peritidal platform-top lithofacies (Urzulei Fm.) and reefal margins (upper Mt. Tului Fm.) was flooded during the late Early Tithonian, and then overlain by pelagic carbonates (Pedra Longa Fm.). The Urzulei and Pedra Longa units are absent in the Mt. Albo area, confirming a more monotonous environmental evolution for the northern area (Fig. 3). For this reason, the stratigraphic boundary between the Mt. Tului and Bardia formations results controversial. In agreement with Jadoul et al. (2010), this study considers:

a) Mt. Tului Fm. as a shallow-water platform/ramp coeval to the S'Adde Lms. (and Baunei Fm.), spanning the same interval between Callovian hardgrounds and the Lower/Upper Tithonian transgressive Pedra Longa Fm. (Fig. 3);

b) the lower Mt. Bardia Fm. including the Upper Tithonian progradational reef complex (Lanfranchi et al. 2011);

c) the upper Mt. Bardia Fm. comprising the Berriasian open shelf, back-reef to inner platform widely outcropping in the Mt. Albo and in the costal massif between Mt. Tuttavista and Baunei.

The different Tithonian evolution between the north and south basins may depend on different subsidence/accommodation trends that in turn can reflect different tectonic settings of the Eastern Sardinian passive margin during the Early/Late Tithonian transition.

Conclusions

– The chronostratigraphy of S'Adde Lms. has been revised: the lowermost Lithozone 1 is Late Bathonian-earliest Callovian; the Lithozone 2 is Callovian-possibly EarlyKimmeridgian; the Lithozone 3 is Late Kimmeridgian-Early Tithonian. On the basis of the data presented here, the formalization of the S'Adde Limestone is proposed: it includes the *S'Adde Limestone* (Dieni & Massari 1985), and the dolomitized thin bedded pelagic limestone previously attributed to the Dorgali Formation. The presented results confirm that the studied section of the S'Adde valley (Mt. Albo) may be considered the type-section of the S'Adde Limestone.

– A regional small scale tensional tectonic activity (Late Bathonian to Early Oxfordian) played a role in delineating the Middle-Late Jurassic basin-and-swell setting in the north Mt. Albo area, contributing to subsidence and/or high sedimentation rates in the S'Adde basin, and favouring the Callovian condensation on the Posada-Siniscola-Cuile sa Funtana swell, and the development of the shallow-water carbonate ramps of Mt. Tului and lower Mt. Bardia formations.

– The litho-bio-chronological data set achieved here permits to integrate the evolution of the Eastern Sardinian passive margin in the wider framework of the southern European passive margin during the Middle-Late Jurassic. The Upper Bathonian-Callovian and Oxfordian deposits are condensed interval displaying affinities with the entire southern European margin that was subjected to a pronounced reduction of sediment production during these times. All these cases are framed in time slices of global changes in carbonate production/sedimentation probably linked to climate changes, oscillations in sea-level, and reorganisation of oceanic currents.

Acknowledgments. This work benefited of the careful and accurate revisions of E. Mattioli, F. Massari and I. Dieni, who greatly improved both the overall structure of the manuscript as well as the English form. We would like to acknowledge G. Della Porta for useful discussions and precious suggestions on the English language.

This study has been supported by MIUR-COFIN 2008NWTC3Z_002 to F. Jadoul.

REFERENCES

Abbink O., Targarona J., Brinkhuis H. & Visscher H. (2001) - Late Jurassic to earliest Cretaceous paleoclimatic evolution of the southern North Sea. *Global Planet. Change,* 30: 231-256.

Amadesi E., Cantelli C., Carloni G.C. & Rabbi E. (1961) - Carta geologica del Foglio 208-Dorgali, 1:100.000, Libreria dello Stato, Roma.

Aurell M., Robles S., Bàdenas B., Rosales I., Quesada I., Meléndez G. & Garci'a-Ramos J.C. (2003) - Transgressive-regressive cycles and Jurassic palaeogeography of northeast Iberia. *Sediment. Geol.,* 162: 239-271.

Azéma J., Chabrier G., Fourcade E. & Jaffrezo M. (1977) - Nouvelles donnée micropaléontologiques, stratigraphiques et paléogeographiques sur le Portlandien et le Néocomien de Sardaigne. *Rev. Micropal.*, 20: 125-139.

Azerêdo A.C., Wright V.P. & Ramalho M. (2002) - The Middle-Late Jurassic forced regression and disconformity in central Portugal: eustatic, tectonic and climatic effects on a carbonate ramp system. *Sedimentology,* 49: 1339-1370.

Bernoulli D. & Jenkyns H.C. (1974) - Alpine, Mediterranean, and Central Atlantic Mesozoic facies in relation to the early evolution of the Tethys. In: Dott R.H. & Shaver R.H. (Eds) - Modern and ancient geosynclinal sedimentation. *SEPM Sp. Publ.*, 19: 129-159.

Bernoulli D. & Jenkyns H.C. (2009) - Ancient oceans and continental margins of the Alpine-Mediterranean Tethys: deciphering clues from Mesozoic pelagic sediments and ophiolites. *Sedimentology,* 56(1): 149-190.

Bown P.R. (1998) - Calcareous nannofossil biostratigraphy. V. of 315 pp., Kluwer Academic Publishers.

Bralower T.J., Monechi S. & Thierstein H.R. (1989) - Calcareous nannofossils Zonation of the Jurassic-Cretaceous Boundary interval and correlations with the Geomagnetic Polarity Timescale. *Mar. Micropaleontol.,* 14: 153-235.

Calvino F., Dieni I., Ferasin F. & Piccoli G. (1972) - Carta geologica del Foglio 195-Orosei, 1:100.000, Libreria dello Stato, Roma.

Carmignani L. (2001) - Geologia della Sardegna, Note illustrative della Carta Geologica della Sardegna a scala 1:200.000. *Mem. descr. Carta Geol. It.,* Vol. LX, 283 pp. IPZS, Roma.

Carpentier C., Lathuilière B. & Ferry S. (2010) - Sequential and climatic framework of the growth and demise of a carbonatee platform: implications for the peritidal cycles (Late Jurassic, North-eastern France). *Sedimentology*, 57: 985-1020.

Casellato C.E. (2010) - Calcareous nannofossil biostratigraphy of Upper Callovian-Lower Berriasian successions from Southern Alps, North Italy. *Riv. It. Paleont. Strat.*, 116(3): 357-404.

Colombié C. & Rameil N. (2007) - Tethyan-to-boreal correlation in the Kimmeridgian using high-resolution sequence stratigraphy (Vocontian Basin, Swiss Jura, Boulonnais, Dorset). *Int. J. Earth Sci.,* 96: 567-591.

Costamagna L.G. & Barca S. (2004) - Stratigrafia, analisi di facies, paleogeografia ed inquadramento regionale del Giurassico dell'area dei Tacchi (Sardegna centro-orientale). *Boll. Soc. Geol. Ital*., 123: 477-495.

Costamagna L.G., Barca S. & Lecca L. (2007) - The Bajocian-Kimmeridgian Jurassic sedimentary cycle of eastern Sardinia: Stratigraphic, depositional and sequence interpretation of the new 'Baunei Group'. *C.R. Geoscience*, 339: 601-612.

Corbin J.-C., Person A., Iatzoura A., Ferré B. & Renard M. (2000) - Manganese in pelagic carbonates: indication of major tectonic events during the geodynamic evolution of a passive continental margin (the Jurassic European Margin of the Tethys-Ligurian Sea). *Palaeogeogr. Palaeoclimatol. Palaeoecol.,* 156: 123-138.

Dercourt J., Gaetani M., Vrielynck B., Barrier E., Biju-Duval B., Brunet M.F., Cadet J.P., Crasquin S. & Sandulescu M. (2000) - Atlas Peri-Tethys, Palaeogeographical Maps. V. of 1-269 pp. CCGM/CGMW, Paris, 24 maps and explanatory notes: I-XX.

Dieni I. & Massari F. (1985) - Mesozoic of Eastern Sardinia. In: Cherchi A. (Ed.) - 19th European Micropaleontological Colloquium. Sardinia October 1-10, 1985. Micropaleontological researches in Sardinia. Guidebook: 66-77.

Dieni I. & Radoičić R. (1999) - *Clypeina dragastani* sp. nov., *Salpingoporella granieri* sp. nov. and other dasycladalean algae from the Berriasian of Eastern Sardinia. *Acta Palaeontol. Rom.,* 2: 105-123.

Dieni I., Massari F. & Sturani C. (1966) - Segnalazione di ammoniti nel Giurese della Sardegna orientale. *Acc. Naz. Lin*., 40: 99-107.

Dieni I., Massari F. & Médus J. (2008) - Age, depositional environment and stratigraphic value of the Cuccuru 'e Flores Conglomerate: insight into the Palaeogene to Early Miocene geodynamic evolution of Sardinia. *Bull. Soc. Géol. France*, 179: 51-72.

Dieni I., Fischer J.C., Massari F., Salard-Cheboldaeff M. &Vozenin-Serra C. (1983) - La sucession de Genna Selole (Baunei) dans le cadre de la palégéographie mésojurassique de la Sardaigne oriental. *Mem. Soc. Geol. It.,* 36: 117-148.

Dromart G., Garcia J.P., Picard S., Atrops F., Lecuyer C. & Sheppard S.M.F. (2003) - Ice age at the Middle-Late Jurassic transition? *Earth Planet. Sci. Lett.,* 213: 205-220.

Erba E. & Casellato C.E. (2010) - Paleoceanografia del Giurassico nella Tetide occidentale: l'archivio geologico del Bacino Lombardo. *Rendiconti dell'Istituto Lombardo, Accademia di Scienze e Lettere*. Special Publication on "Una nuova Geologia per la Lombardia", 447: 115-140.

Fourcade E., Azema J., Chabrier G., Chauve P., Foucault A. & Rangheard Y. (1977) - Liaisons paléógéographiques au Mésozoïque entre les zones externes bétiques, baléares, corso-sardes et alpines. *Rev. Géogr. Phys. Géol. Dyn*., 19: 377-388.

Fourcade E., Azema J., Cecca F., Dercourt J., Vrielynck B., Bellion Y., Sandulescu M. & Ricou L.E. (1993) - Late Tithonian Palaeoenvironments (138 to 145 Ma). In: Dercourt J., Ricou L.E. & Vriekynck B. (Eds) - Atlas Tethys Palaeoenvironmental Maps. BEICIP-FRANLAB, Rueil-Malmaison.

Garzanti E., Haas R. & Jadoul F. (1989) - Ironstones in the Mesozoic passive margin sequence of the Tethys Himalaya (Zanskar, Northern India): sedimentology and metamorphism. In: Young T.P. & Taylor W.E.G. (Eds) - Phanerozoic Ironstones. *Geol. Soc. Sp. Publ.,* 46: 229-244.

Giusberti L. & Coccioni R. (2003) - *Posadia feroniensis* n. gen., n. sp. (*Lituolida, Hormosinidae*) from the Bathonian of Sardinia, Italy. *J. Foram. Res.,* 33(3): 211-218.

Gómez J.J. & Fernández-López S.R. (2006) - The Iberian Middle Jurassic carbonate-platform system: Synthesis of the paleogeographic elements of its eastern margin (Spain). *Palaeogeogr. Palaeoclimatol. Palaeoecol.,* 236: 190-205.

Jadoul F., Lanfranchi A., Casellato C.E., Berra F. & Galli M.T. (2007) - Stratigraphic evolution and paleogeographic setting of the Middle Jurassic-Early Cretaceous carbonate platforms in Eastern Sardinia (Italy). EGU General Assembly 2007, April, 15-20, Vienna (Austria). *Geophys. Res. Abstracts*, 9, 04411, 2007. SRef-ID: 1607-7962/gra/EGU2007-A-04411.

Jadoul F., Lanfranchi A. & Berra F. (2009) - Evolution of Late Jurassic to Berriasian carbonate platform of Eastern Sardinia. Field Trip N.4, IAS Regional Meeting Alghero 2009, Italy.

Jadoul F., Lanfranchi A., Berra F., Erba E., Casellato C.E., Cherchi A., Simone L., Schroeder R., Carannante G. & Ibba A. (2010) - I sistemi giurassici della Sardegna orientale (Golfo di Orosei) ed eventi deposizionali nel sistema carbonatico giurassico-cretacico della Nurra (Sardegna nord-occidentale). 84° Congresso nazionale della Società Italiana - Sassari, 2008 - Escursione E05. Geol. F. Trips, 2(2.1), 122 pp. Prima parte DOI 10.3301/GFT.2010.02, Seconda parte DOI 10.3301/GFT.2010.03.

Jenkyns H.C., Jones C.E., Groecke D.R., Hesselbo S.P. & Parknson D.N. (2002) - Chemostratigraphy of the Jurassic System: application, limitations and implication for paleoceanography. *J. Geol. Soc. London,* 159: 351-378.

Lanfranchi A. (2009) - Stratigraphy, palaeogeography and facies analysis of Upper Jurassic-Berriasian carbonate depositional systems of eastern Sardinia. Ph.D. Thesis, Università degli Studi di Milano, Ciclo XXI, 129 pp.

Lanfranchi A., Canavesi M., Casellato C.E., Jadoul F., Cherchi A., Schroeder R. & Berra F. (2008) - Stratigraphy, facies analysis and paleogeography of the Late Jurassic "Urzulei Formation" (Eastern Sardinia). *Rend. online Soc. Geol. It.,* 3: 484-485.

Lanfranchi A., Berra F. & Jadoul F. (2011) - Compositional changes in sigmoidal carbonate clinoforms (Late Tithonian, eastern Sardinia, Italy): insights from quantitative microfacies analyses. *Sedimentology,* 58: 2039-2060.

Lohmann H. (1902) - Die Coccolithophoridae, eine Monographie der coccolithen-bildenden Flagellaten, zugleich ein Beitrag zur Kenntnis des Mittelmeerauftriebs. *Archiv für Protistenkunde*, 1: 89-165.

Louis-Schmid B., Rais P., Bernasconi S.M., Pellenard P., Collin P.Y. & Weissert H. (2007) - Detailed record of the mid-Oxfordian (Late Jurassic) positive carbon-isotope excursion in two hemipelagic section (France and Switzerland): A plate tectonic trigger? *Palaeogeogr. Palaeoclimatol. Palaeoecol.*, 248(3-4): 459-472.

Massari F. & Dieni I. (1983) - Pelagic oncoids and ooids in the Middle-Upper Jurassic of Eastern Sardinia. In: Peryt T.M. (Ed.) - Coated grains: 367-376. Springer-Verlag Berlin Heidelberg.

Masse J.-P. & Allemann J. (1982) - Relations entre les séries carbonatées de plate-forme provençale et sarde au Crétacé inférieur. *Cret. Res*., 3: 19-33.

Mattioli E. & Erba E. (1999) - Synthesis of calcareous nannofossil events in tethyan Lower and Middle Jurassic successions. *Riv. It. Paleont. Strat*., 105(3): 343-376.

Monleau C. (1986) - Le Jurassique inférieur et moyen de Provence, Sardaigne et Alpes Maritimes: corrélation, essai de synthè- se paléogéographique. *Rev. Géol. Dyn. Géo. Phys.*, 27: 3-11.

Padden M., Weissert H. & de Rafelis M. (2001) - Evidence for Late Jurassic release of methane from gas hydrate. *Geology,* 29(3): 223-226.

Pasci S., Oggiano G. & Funedda A. (1998) - Rapporti tra tettonica e sedimentazione lungo le fasce trascorrenti oligo-aquitaniane della Sardegna NE. *Boll. Soc. Geol. It.*, 117: 443-453.

Ramajo J. & Aurell M. (2008) - Long-term Callovian-Oxfordian sea-level changes and sedimentation in the Iberian carbonate platform (Jurassic, Spain): possible eustatic implications. *Basin Res.*, 20: 163-184.

Rameil N. (2005) - Carbonate sedimentology, sequence stratigraphy and chronostratigraphy of the Tithonian in the Swiss and French Jura Mountains: a high-resolution records of changes in sea-level and climate. *Geofocus,* 13: 1-126.

Randisi A., Ferreri V., D'Argenio B. & Bravi S. (2008) - Cyclic organization of Late Jurassic carbonate platform strata. Matese mountains, southern Apennines. *Boll. Soc. Geol. It.*, 127: 429-438.

Reale V. & Monechi S. (1994) - *Cyclagelosphaera wiedmannii* new species, a marker for the Callovian. *J. Nannoplankton Res.*, 16(3): 117-119.

Reolid M., Nieto L.M. & Rey J. (2010) - Taphonomy of cephalopod assemblages from Middle Jurassic hardgrounds of pelagic swells (South-Iberian Paleomargin, Western Tethys). *Palaeogeogr. Palaeoclimatol. Palaeoecol.,* 292: 257-271.

Ricci C., Jadoul F., Lanfranchi A., Rusciadelli G., Della Porta G., Lathuilière B. & Berra F. (2012) - Coral-sponge-microencruster-microbialite associations in the Upper Jurassic reef: quantitative characterization of a case study from Eastern Sardinia (Italy). 86° Congresso Nazionale della Società Geologica Italiana, Arcavacata di Rende (CS), 18-20 Settembre 2012.

Roth P.H. (1983) - Jurassic and Lower Cretaceous calcareous nannofossil in the Western North Atlantic (Site 534): biostratigraphy, preservation and some observation on biogeography and paleoceanography. *Init. Rep. DSDP,* 76: 587-621.

Roth P.H. (1986) - Mesozoic paleoceanography of the North Atlantic and Tethys Oceans. In: Summerhays C.P. & Shackleton N.J. (Eds) - North Atlantic Paleoceanography. *Geol. Soc. Sp. Publ.*, 26: 299-320.

Roth P.H. (1989) - Ocean circulation and calcareous nannoplankton evolution during the Jurassic and Cretaceous. *Palaeogeogr. Palaeoclimatol. Palaeoecol.,* 74: 111-126.

Rusciadelli G., D'Argenio B., Di Simone S., Ferreri V., Randisi A. & Ricci C. (2009) - Carbonate platform production and exportation potentials recorded by stratigraphic architectures and sediment composition of base-of-slope deposits (Late Jurassic, central Apennines, Italy). In: Kneller B., Martinsen O.J. & McCaffrey B. (Eds) - External Controls on Deep-Water Depositional Systems. *SEPM Sp. Publ.*, 92: 279-30.

Santantonio M. (1993) - Facies association and evolution of pelagic carbonate platform/basin system: Examples from Italian Jurassic. *Sedimentology*, 40: 1039-1067. doi: 10.1111/j.1365-3091.1993.tb01379.x.

Santantonio M. & Teale C.T. (1985) - Jurassic condensed sedimentation on Hercynian basement (Calabria, Italy). In: Rosell J., Remacha E. & Zamorano M. (Eds) - Abstracts of the 6th European Meeting of the International Association of Sedimentologists, Lerida: 4459-460.

Schlager W., Reijmer J.J.G. & Droxler A. (1994) - Highstand shedding of carbonate platform. *J. Sed. Res.*, B64(3): 270-281.

Tisljar J. & Velic I. (1993) - Upper Jurassic (Malm) shallow-water carbonates in the Western Gorski Kotar area: facies and depositional environments (Western Croatia). *Geol. Croat.,* 46: 263-279.

Vardabasso S. (1959) - Il Mesozoico epicontinentale della Sardegna. *Rend. Sc. Fis. Mat. e Nat.*, 27: 178-184.

Védrine S. & Strasser A. (2009) - High-frequency paleoenvironmental changes on a shallow carbonate platform during a marine transgression (Late Oxfordian, Swiss Jura Mountains). *Swiss. J. Geosci.*, 102: 247-270.

Vörös A. (2011) - Episodic sedimentation on a peri-Tethyan ridge through the Middle-Late Jurassic transition (Villàny Mountains, southern Hungary). *Facies*, doi: 10.1007/s10347-011-0287-8.

Weissert H. & Erba E. (2004) - Volcanism, CO_2 and palaeoclimate: a Late Jurassic - Early Cretaceous carbon and oxygen isotope record. *J. Geol. Soc., London*, 161: 1-8.

Appendix 1

Tables report SEM-EDS semiquantitative analyses carried out on carbon coated thin sections (sample J4a and J5) from HG-2 of Siniscola section (Fig. 9G-H). Analyses have been performed to obtain the elemental composition of selected points of the coating surrounding quartz extraclasts.

SAMPLE J4	Element	App. Concentr.	Fit Index	Element %	Sigma %	Atomic %	Compound %	
Point 15	Na	0,5525	73,5000	1,1258	0,1270	1,9878	Na2O	1,5175
	Mg	0,4615	2,8056	0,9248	0,0886	1,5441	MgO	1,5334
	Al	0,9937	0,2162	1,6439	0,0844	2,4731	Al2O3	3,1059
	Si	1,8536	0,3077	2,4611	0,0807	3,5571	SiO2	5,2650
	P	1,2716	0,4762	1,1784	0,0772	1,5444	P2O5	2,7002
	Cl	0,0791	0,1957	0,0857	0,0523	0,0981		0,0000
	K	0,2494	0,2308	0,2335	0,0547	0,2424	K2O	0,2813
	Ca	3,0254	0,3214	2,9774	0,0851	3,0155	CaO	4,1659
	Ti	0,9838	0,2344	1,0305	0,0812	0,8733	TiO2	1,7188
	Fe	39,4871	2,2125	43,0326	0,4457	31,2790	FeO	55,3606
	O			21,0406	0,3115	53,3852		
Point 16	Na	0,3364	52,2059	0,6937	0,1108	1,2542	Na2O	0,9351
	Mg	0,3143	1,2778	0,6323	0,0770	1,0809	MgO	1,0483
	Al	0,6231	0,1081	1,0296	0,0727	1,5860	Al2O3	1,9453
	Si	1,5462	0,2051	2,0336	0,0735	3,0095	SiO2	4,3504
	P	1,4813	1,7857	1,3547	0,0747	1,8179	P2O5	3,1041
	Cl	0,0621	0,5870	0,0667	0,0496	0,0783		0,0000
	K	0,1205	0,2115	0,1118	0,0538	0,1189	K2O	0,1347
	Ca	4,5457	0,4286	4,4494	0,0997	4,6142	CaO	6,2255
	Ti	0,9323	0,3906	0,9816	0,0805	0,8518	TiO2	1,6373
	Fe	39,8192	3,3125	43,3726	0,4457	32,2802	FeO	55,7980
	O			20,5194	0,3034	53,3081		
Point 17	Na	0,4131	77,2353	0,8685	0,1289	1,5604	Na2O	1,1707
	Mg	0,3485	2,3889	0,7146	0,0889	1,2141	MgO	1,1848
	Al	0,8807	0,2703	1,4802	0,0843	2,2661	Al2O3	2,7968
	Si	1,9747	0,5641	2,6478	0,0825	3,8942	SiO2	5,6644
	P	0,5655	1,1667	0,5285	0,0707	0,7049	P2O5	1,2111
	Cl	0,0312	0,4565	0,0337	0,0530	0,0393		0,0000
	K	0,1824	0,4038	0,1702	0,0547	0,1798	K2O	0,2050
	Ca	1,3533	0,5179	1,3206	0,0716	1,3610	CaO	1,8477
	Ti	0,8985	0,8906	0,9184	0,0797	0,7920	TiO2	1,5320
	Fe	43,8635	1,2125	47,3269	0,4645	35,0048	FeO	60,8850
	O			20,5218	0,3166	52,9836		
Point 18	Na	0,4557	73,2353	0,9219	0,1267	1,6194	Na2O	1,2426
	Mg	0,4085	2,0278	0,8112	0,0889	1,3476	MgO	1,3451
	Al	1,1864	0,1892	1,9455	0,0878	2,9120	Al2O3	3,6759
	Si	2,5965	0,1026	3,4399	0,0886	4,9465	SiO2	7,3590
	P	1,0543	0,7381	0,9883	0,0775	1,2886	P2O5	2,2645
	Cl	0,0543	0,3261	0,0592	0,0511	0,0675		0,0000
	K	0,4925	0,3269	0,4640	0,0592	0,4792	K2O	0,5589
	Ca	2,0835	0,4821	2,0627	0,0787	2,0785	CaO	2,8861
	Ti	0,9178	0,2031	0,9606	0,0778	0,8100	TiO2	1,6024
	Fe	38,5722	1,0125	42,0883	0,4415	30,4366	FeO	54,1458
	O			21,3977	0,3121	54,0143		
Point 19	Na	0,4648	70,0000	0,9545	0,1203	1,6892	Na2O	1,2866
	Mg	0,3881	2,3611	0,7808	0,0821	1,3068	MgO	1,2947
	Al	0,8658	0,0541	1,4337	0,0796	2,1620	Al2O3	2,7088
	Si	1,5876	0,0513	2,1026	0,0776	3,0460	SiO2	4,4981
	P	1,5421	1,5238	1,4193	0,0781	1,8644	P2O5	3,2521
	Cl	0,0150	0,1957	0,0162	0,0516	0,0186		0,0000
	K	(0,0564)	0,0962	(0,0526)	0,0540	(0,0547)	K2O	(0,0633)
	Ca	3,5545	0,1071	3,4821	0,0910	3,5350	CaO	4,8721
	Ti	1,1192	0,4844	1,1715	0,0811	0,9951	TiO2	1,9541
	Fe	40,2116	1,4875	43,7792	0,4495	31,8960	FeO	56,3211
	O			21,0530	0,3099	53,5415		
Point 20	Na	0,3412	68,8824	0,7034	0,1157	1,2422	Na2O	0,9482
	Mg	0,4079	1,7222	0,8208	0,0841	1,3707	MgO	1,3610
	Al	1,1970	0,1351	1,9848	0,0871	2,9863	Al2O3	3,7501
	Si	3,1918	0,0769	4,2683	0,0910	6,1697	SiO2	9,1311
	P	0,2392	0,1190	0,2280	0,0659	0,2988	P2O5	0,5223
	Cl	0,0117	0,1522	0,0128	0,0508	0,0147		0,0000
	K	0,5410	0,6154	0,5107	0,0612	0,5302	K2O	0,6152
	Ca	0,4162	0,2321	0,4112	0,0599	0,4165	CaO	0,5753
	Ti	0,4827	0,2656	0,4959	0,0714	0,4203	TiO2	0,8272
	Fe	41,5528	0,6625	45,0318	0,4531	32,7354	FeO	57,9324
	O			21,2080	0,3091	53,8152		
Point 21	Na	0,2772	56,5588	0,5969	0,1130	1,1444	Na2O	0,8046
	Mg	0,2576	1,8889	0,5374	0,0785	0,9744	MgO	0,8911
	Al	0,6228	0,1351	1,0593	0,0749	1,7304	Al2O3	2,0014
	Si	1,6914	0,1795	2,2774	0,0754	3,5741	SiO2	4,8721
	P	0,2556	0,5476	0,2386	0,0622	0,3395	P2O5	0,5467
	Cl	0,0279	0,3696	0,0300	0,0508	0,0373		0,0000
	K	0,1668	0,4808	0,1548	0,0546	0,1745	K2O	0,1865
	Ca	0,7875	0,5000	0,7630	0,0647	0,8391	CaO	1,0676
	Ti	0,6417	1,0938	0,6465	0,0749	0,5949	TiO2	1,0784
	Fe	45,1436	1,1500	48,3599	0,4663	38,1680	FeO	62,2140
	O			19,0285	0,3054	52,4234		
Point 22	Na	0,2435	49,7647	0,5284	0,0975	1,0113	Na2O	0,7123
	Mg	0,2373	1,0833	0,4981	0,0697	0,9013	MgO	0,8258
	Al	0,5714	0,0541	0,9760	0,0693	1,5916	Al2O3	1,8441
	Si	1,6537	0,0513	2,2313	0,0725	3,4955	SiO2	4,7734
	P	0,1088	0,2857	0,1016	0,0596	0,1443	P2O5	0,2328
	Cl	0,0644	0,1739	0,0691	0,0487	0,0857		0,0000
	K	0,2490	0,3654	0,2308	0,0545	0,2597	K2O	0,2780
	Ca	0,5223	0,4286	0,5052	0,0610	0,5546	CaO	0,7069
	Ti	0,4493	0,2813	0,4501	0,0697	0,4134	TiO2	0,7508
	Fe	46,8670	0,9000	50,0640	0,4740	39,4426	FeO	64,4063
	O			18,9449	0,3018	52,1000		

S'adde Valley section studied samples **(1)**	**PRESERVATION**	**TOTAL ABUNDANCE**	*P. cf. enigma*	*S. punctulata*	*W. barnesiae*	*W. manivitiae*	*W. manivitiae* LARGE	*W. communis*	*W. fossacincta*	*W. britannica*	*L. hauffii*	*L. sigillatus*	*L. cf. crucicentralis*	*W. britannica* LARGE	*C. margerelii*	*C. wiedmannii*	*W. communis* LARGE	*M. quadratus*	*Z. erectus*	*C. deflandrei*	*F. multicolumnatus*	*C. tubulata*	*C. crassus*	*D. lehmanii*	*Z. fluxus*	*C. mexicana minor*	*Z. embergeri*	*C. mexicana mexicana*	**BIOZONES - Casellato, 2010**
S180	u.m.	~B			R																R								NJT 15a
S178	u.m.	~B			R																R								
S175	u.m.	RR				R			R												R								
S171	u.m.	B													BARREN														
S159	u.m.	~B																										R	
S151	u.m.	~B								R																		R	
S132	-	B													BARREN														
S127	-	B													BARREN														
S126	E3-O1	RR			R				R	R							R												
S125	-	~B																			R								
S123	E2-O2	RR																			R					R		?	
S121	E1-O1	R			R	R		R	R	R				R	R					R	R				R	R			
S119	E1-O1	R		R	R	R		R	R	R					R						F		R	R		R	R		
S118	E1-O2	R		R	R	R		R													R					R			
S117	E3	RR			R									R							R					R			
S116	E2-O2	RR			R					R										R	R								NJT 14
S115	E2-O1	R			R	R		R		R				R	R					?									
S114	E3-O3	RR			R		R								R					?	R								
S113	E1/2-O2	R			R	R	R	R	R	R					R														
S112	E2-O2	R			R	R	R	R							R		R												
S111	E2-O2	RR		R	R		R	R							R						?								
S110	E2-O2/3	R		R	R	R	R								R						R								
S109	E2-O1	R		?	R	R		R	R	R					R					R	R								
S108	E3-O1	RR			R					R					R						?								
S107	E3-O2	RR								R										R									
S106	E3-O3	RR		R	R																R								
S105	E3-O3	RR					R	R																					
S104	E3-O2	RR			R	R									R						R								
S103	E2-O1	RR		R				R																					
S102	-	~B					R																						
S101	-	~B												R							R								
S100	E2-O2	RR			R			R							R						R								
S99	E3-O3	RR		R	R			R		R																			
S98	E3-O3	RR			R			R		R					R						R								
S97	E3-O2	R		R	R	R				R				R	R					R	R								
S96	E2-O1	R		R	R	R		R	R	R					R					R	R			R					
S95	E2-O1	R		R	R	R		R							R					R	R								
S94	E2-O2	R		R	R	R	R	R						R	R						R								
S93	E3-O2	RR			R			R							R														
S92	E3-O2	RR																		R	R								
S91	E3-O2	R		R	R	R	R	R		R					R					R									
S90	E2-O2	R			R		R			R				R						R	R								
S89	E3-O1/2	R			R	R	R	R		R				R					R		R				R				
S88	E3-O2	RR		R	R	R				R					R														
S87	E1-O1	R			R	R	R	R		R					R						R								
S86	E1-O2	RR		R	R	R								R	R														
S85	E1-O2/3	R		R	R	R		R		R				R	R		R			R	R								
S84	E1/2-O1	R		R	R	R	R	R	R	R							R												
S83	E1-O2	R		R	R	R		R							R		R	?			R		R						
S82	E1-O2	R		R	R	R	R	R							R			R		R	R								
S81	E2-O2	R		R	R	R		R		R					R			R		R	R								
S78	E3-O1	RR		R				R									R				R								
S77	E2-O2	R		R	R	R	R	R	R	R							R			R	R								
S76	-	~B				R									R														
S74	E1-O2	R		R	R		R	R	R	R				R	R					R	R		R	R					
S73	E1-O2	RR				R	R	R		R					R		R			?									
S72	E1-O2	RR		R	R		R	R	R						R														
S71	E1-O1/2	RR		R	R	R	R							R	R		R												
S70	E1-O1/2	RR		R				R		R				R	R					?			R						
S69	E1-O1/2	RR			R		R	R		R							R			R									
S68	E1-O1/2	R		R	R	R	R	R	R					R	R					R									
S67	E2-O2/3	RR			R		R	R		R					R						R								

S'adde Valley section studied samples (2)	**PRESERVATION**	**TOTAL ABUNDANCE**	*P. cf. enigma*	*S. punctulata*	*W. barnesiae*	*W. manivitiae*	*W. manivitiae* LARGE	*W. communis*	*W. fossacincta*	*W. britannica*	*L. hauffii*	*L. sigillatus*	*L. cf. crucicentralis*	*W. britannica* LARGE	*C. margerelii*	*C. wiedmannii*	*W. communis* LARGE	*M. quadratus*	*Z. erectus*	*C. deflandrei*	*F. multicolumnatus*	*C. tubulata*	*C. crassus*	*D. lehmanii*	*Z. fluxus*	*C. mexicana minor*	*Z. erbergeri*	*C. mexicana mexicana*	**BIOZONES - Casellato, 2010**
S66	E1-O1/2	R			R	R	R			R					R														
S65	E2/3-O2/3	RR								R											R								
S64	E1/2-O2	RR		R	R	R	R			R												R							
S63	-	B													BARREN														
S62	E1/2-O2	R		R	R	R	R	R		R					R		R				R								
S61	E2-O2/3	RR		R	R	R									R			?	R		R								
S60	E2-O2/3	R		R	R	R	R	R										?		R	R								
S58	E2/3-O2/3	RR			R		R			R								?											
S57	E2-O2	R		R	R	R	R	R		R				R				?			R								
S56	E1-O2	R		R	R			R							R						R								NJT 14
S55	E2-O3	RR		R	R	R	R	R	R						R			?			R								
S54	E2-O2	R			R	R	R	R	R	R					R			R		?	R								
S53	E2/3-O2/3	R/F		R	R	R	R	R		R	R			R	R					R									
S52	E2-O2/3	F		R	F	R	R	R		R				R	R			R		R	R								
S51	E2-O3	R		R	R		R	R		R				R	R														
S50	-	~B			R										R														
S49	E2/3-O3	R		R	R	R	R	R		R				R	R														
S48	E2-O2	RR		R		R		R	R	R																			
S47	E2-O2	R			R			R	R	R	R		?		R						R								
S46	E2-O2	R			R	R	R	R		R					R			?		R									
S45	E3-O3	RR		R			R			R										R									
S44	E2-O2	R		R	R	R	R	R		R				R	R														
S43	E2-O2	R		R	R	R		R		R					R				R	R									NJT 13b
S42	E2/3-O3	R		R	R		R	R		R					R					R									
S41	E2/3-O2/3	R			R	R	R	R		R	R			R			R	R											
S40	E3-O2/3	R		R		R	R	R	R		R			R															
S39	E2-O1/2	R		R	R	R	R	R		R	R	R			R														
S38	E2-O2	R			R		R	R		R				R	R														NJT 13a
S37	E2-O2	R			R	R	R	R		R				R			R												
S36	E2-O2	R		R	R	R		R		R				R	R	R	R												
S35	E1-O2/3	R		R	R	R	R	R	R	R		R	?	R	R														
S34	E2-O1	R		R	R	R	R	R	R	R				R	R	R	R												
S33	E2-O2	R			R	R	R	R	R	R			?	R		?	R												
S32	E2-O2	F	R	R	R	R	R	R	R	R				R	R	?	R												
S31	E3-O1/2	RR		R		R	R	R		R						?													
S29	E2-O2	RR						R		R					R														
S28	E2-O1	RR			R			R	R	R					R	R	R												
S27	E2-O2	RR	R	R	R											R													
S26	E2-O2	R/F	R	R	R	R	R	R	R	R				R	R	R													
S25	E1-O2	R		R	R		R			R					R	R													
S24	E2-O2	R		R	R	R	R	R		R			R	R	R	R													
S23	E3-O2	RR			R		R			R						R													
S22b	E2-O2	RR			R		R			R																			
S22	E2-O2	RR			R	R	R					R				R													NJT 12
S21	E2-O1	RR			R					R																			
S20	E3-O1	RR		R																									
S19	E2/3-O1	RR			R						R	R		R	R														
S18	E2-O2	R		R	R		R	R		R					R	R													
S17	E2/3-O2/3	R		R	R		R	R		R						R													
S16	E3-O3	RR			R	R				R				R	R	R	R												
S15b	E3-O3	RR			R																								
S15	E3-O2	RR			R					R	R	R				R													
S12	E2-O2	RR	R		R			R		R				R															
S11	E1-O1/2	R	R	R	R	R	R	R	R	R	R	R			R	R													
S10	-	~B													R														
S8	E2-O2	R			R	R	R	R				R	?		R	R	R												
S7	E2-O1	RR					R	R				R	?		R	R													
S6	E1-O2	R	R		R	R	R	R	R	R	R	R	R	R	R														
S4	-	B													BARREN														NJT 11
S3	E3	RR	R	R																									

Appendix 2

The chart reports the distribution, relative and total abundance estimations as well as preservation evaluation of each taxon observed in the S'Adde section. Question marks correspond to elements that cannot be unequivocally classified but are tentatively assigned to taxon represented by fragments or heavily dissolved specimens. u.m.= unsuitable material.

Appendix 3

Taxonomic index of calcareous nannofossil taxa reported in this study. Genera, species and subspecies are listed in alphabetic order. Authors and date of the original description and, when necessary, emendations are provided. See Bralower et al. (1989), Bown (1998) and Casellato (2010) and references therein for full information regarding taxonomy and authorships.

Conusphaera mexicana (Trejo, 1969) subsp. *mexicana* Bralower in Bralower et al., 1989

Conusphaera mexicana (Trejo, 1969) subsp. *minor* (Bonw & Cooper, 1989) Bralower in Bralower et al., 1989

Crepidolithus crassus (Deflandre in Deflandre & Fert, 1954) Noël, 1965

Cyclagelosphaera deflandrei (Manivit, 1966) Roth, 1973

Cyclagelosphaera margerelii Noël, 1965

Cyclagelosphaera tubulata (Grün & Zweili, 1980) Cooper, 1987

Cyclagelosphaera wiedmannii Reale & Monechi, 1994

Diazomatolithus lehmanii Noël, 1965

Faviconus multicolumnatus Bralower in Bralower et al., 1989

Lotharingius crucicentralis (Medd, 1971) Grün & Zweili, 1980

Lotharingius hauffii Grün & Zweili in Grün et al., 1974

Lotharingius sigillatus (Stradner 1971) Prins in Grün et al., 1974

Microstaurus quadratus Black, 1971

Pseudoconus enigma Bown & Cooper, 1989

Schizosphaerella punctulata Deflandre & Dangeard, 1938

Watznaueria barnesiae (Black in Black & Barnes 1959) Perch-Nielsen, 1968

Watznaueria britannica (Stradner,1963) Reinhardt, 1964

Watznaueria communis Reinhardt, 1964

Watznaueria fossacincta (Black, 1971a) Bown in Bown & Cooper, 1989

Watznaueria manivitiae (Bukry, 1973) Moshkovitz & Ehrlich, 1987

Zeugrhabdotus embergeri (Noël, 1958) Perch-Nielsen, 1984

Zeugrhabdotus erectus (Deflandre in Deflandre & Fert, 1954) Reinhardt, 1965

Zeugrhabdotus fluxus Casellato, 2010